

**DRAFT DELIBERATIVE: FOR INTERAGENCY REVIEW ONLY.
DO NOT DISTRIBUTE OUTSIDE YOUR AGENCY.**



EPA/635/R-14/378
Interagency Review Draft
www.epa.gov/iris

Toxicological Review of *tert*-Butyl Alcohol (*tert*-butanol)

(CASRN 75-65-0)

In Support of Summary Information on the Integrated Risk Information System (IRIS)

Supplemental Information

September 2014

NOTICE

This document is an **Interagency Science Consultation Review Draft**. This information is distributed solely for the purpose of pre-dissemination peer review under applicable information quality guidelines. It has not been formally disseminated by EPA. It does not represent and should not be construed to represent any Agency determination or policy. It is being circulated for review of its technical accuracy and science policy implications.

Integrated Risk Information System
National Center for Environmental Assessment
Office of Research and Development
U.S. Environmental Protection Agency
Washington, DC

DISCLAIMER

This document is a preliminary draft for review purposes only. This information is distributed solely for the purpose of pre-dissemination peer review under applicable information quality guidelines. It has not been formally disseminated by EPA. It does not represent and should not be construed to represent any Agency determination or policy. Mention of trade names or commercial products does not constitute endorsement or recommendation for use.

CONTENTS

APPENDIX A. OTHER AGENCY AND INTERNATIONAL ASSESSMENTS A-1

 A.1. OTHER AGENCY AND INTERNATIONAL ASSESSMENTS A-1

APPENDIX B. INFORMATION IN SUPPORT OF HAZARD IDENTIFICATION AND DOSE-
RESPONSE ANALYSIS..... B-1

 B.1. TOXICOKINETICS B-1

 B.1.1. Absorption..... B-1

 B.1.2. Distribution..... B-1

 B.1.3. Metabolism..... B-2

 B.1.4. Excretion..... B-4

 B.1.5. Physiologically Based Pharmacokinetic Models B-5

 B.2. PBPK MODEL EVALUATION SUMMARY B-9

 B.2.1. Evaluation of Existing *tert*-Butanol Submodels..... B-9

 B.2.2. Modification of Existing *tert*-Butanol Submodels..... B-11

 B.2.3. *tert*-Butanol Model Application..... B-14

 B.2.4. PBPK Model Code..... B-15

 B.3. OTHER PERTINENT TOXICITY INFORMATION..... B-16

 B.3.1. Genotoxicity..... B-16

 B.3.2. Summary..... B-21

APPENDIX C. DOSE-RESPONSE MODELING FOR THE DERIVATION OF REFERENCE
VALUES FOR EFFECTS OTHER THAN CANCER AND THE DERIVATION OF
CANCER RISK ESTIMATES C-1

 C.1. BENCHMARK DOSE MODELING SUMMARY C-1

 C.1.1. Noncancer Endpoints C-1

 C.1.2. Cancer EndpointsC-30

APPENDIX D. SUMMARY OF EXTERNAL PEER REVIEW AND PUBLIC COMMENTS AND
EPA’S DISPOSITION D-1

REFERENCES FOR APPENDICES 1

TABLES

Table A-1. Other Agency and International Assessments.....	A-1
Table B-1. PBPK model physiologic parameters and partition coefficients.....	B-12
Table B-2. Rate constants for <i>tert</i> -butanol determined by optimization of the model with experimental data	B-14
Table B-3. Summary of genotoxicity (both in vitro and in vivo) studies of <i>tert</i> -butanol.....	B-20
Table C-1. Non-cancer endpoints selected for dose-response modeling for <i>tert</i> -butanol	C-2
Table C-2. Summary of BMD modeling results for kidney transitional epithelial hyperplasia in male F344 rats exposed to <i>tert</i> -butanol in drinking water for 2 years (NTP, 1995); BMR = 10% extra risk.	C-3
Table C-3. Summary of BMD modeling results for kidney transitional epithelial hyperplasia in female F344 rats exposed to <i>tert</i> -butanol in drinking water for 2 years (NTP, 1995); BMR = 10% extra risk.....	C-6
Table C-4. Summary of BMD modeling results for relative kidney weights in male F344 rats exposed to <i>tert</i> -butanol in drinking water for 15 months (NTP, 1995); BMR = 10% relative deviation and 1 standard deviation.....	C-9
Table C-5. Summary of BMD modeling results for relative kidney weights in female F344 rats exposed to <i>tert</i> -butanol in drinking water for 15 months (NTP, 1995); BMR = 10% relative deviation and 1 standard deviation.....	C-13
Table C-6. Summary of BMD modeling results for kidney inflammation in female rats exposed to <i>tert</i> -butanol in drinking water for 2 years (NTP, 1995); BMR = 10% extra risk.....	C-16
Table C-7. Summary of BMD modeling results for thyroid follicular cell hyperplasia in male B6C3F1 mice exposed to <i>tert</i> -butanol in drinking water for 2 years (NTP, 1995); BMR = 10% extra risk.....	C-19
Table C-8. Summary of BMD modeling results for thyroid follicular cell hyperplasia in female B6C3F1 mice exposed to <i>tert</i> -butanol in drinking water for 2 years (NTP, 1995); BMR = 10% extra risk.	C-20
Table C-9. Summary of BMD modeling results for absolute kidney weight in male F344 rats exposed to <i>tert</i> -butanol via inhalation for 6 hr/d, 5d/wk for 13 weeks (NTP, 1997); BMR = 10% relative deviation from the mean.	C-23
Table C-10. Summary of BMD modeling results for relative kidney weight in male F344 rats exposed to <i>tert</i> -butanol via inhalation for 6 hr/d, 5d/wk for 13 weeks (NTP, 1997); BMR = 10% relative deviation from the mean.	C-26
Table C-11. Summary of BMD modeling results for absolute kidney weight in female F344 rats exposed to <i>tert</i> -butanol via inhalation for 6 hr/d, 5d/wk for 13 weeks (NTP, 1997); BMR = 10% relative deviation from the mean.....	C-29
Table C-12. Summary of BMD modeling results for relative kidney weight in female F344 rats exposed to <i>tert</i> -butanol via inhalation for 6 hrs/d, 5d/wk for 13 weeks (NTP, 1997); BMR = 10% relative deviation from the mean.....	C-30
Table C-13. Cancer endpoints selected for dose-response modeling for <i>tert</i> -butanol.....	C-31
Table C-14. Summary of BMD modeling results for renal tubule adenoma or carcinoma in male F344 rats exposed to <i>tert</i> -butanol in drinking water for 2 years modeled with administered dose units and including all dose groups (NTP, 1995); BMR = 10% extra risk.....	C-32
Table C-15. Summary of BMD modeling results for renal tubule adenoma or carcinoma in male F344 rats exposed to <i>tert</i> -butanol in drinking water for 2 years modeled with administered dose units and excluding high-dose group (NTP, 1995); BMR = 10% extra risk.....	C-34

Table C-16. Summary of BMD modeling results for renal tubule adenoma or carcinoma in male F344 rats exposed to <i>tert</i> -butanol in drinking water for 2 years modeled with PBPK (<i>tert</i> -butanol, mg/L) dose units and including all dose groups (NTP, 1995); BMR = 10% extra risk.....	C-36
Table C-17. Summary of BMD modeling results for renal tubule adenoma or carcinoma in male F344 rats exposed to <i>tert</i> -butanol in drinking water for 2 years modeled with PBPK (<i>tert</i> -butanol, mg/L) dose units and excluding high-dose group (NTP, 1995); BMR = 10% extra risk.	C-38
Table C-18. Summary of BMD modeling results for renal tubule adenoma or carcinoma in male F344 rats exposed to <i>tert</i> -butanol in drinking water for 2 years modeled with PBPK (metabolized, mg/hr) dose units and including all dose groups (NTP, 1995); BMR = 10% extra risk.	C-40
Table C-19. Summary of BMD modeling results for renal tubule adenoma or carcinoma in male F344 rats exposed to <i>tert</i> -butanol in drinking water for 2 years modeled with PBPK (metabolized, mg/hr) dose units and excluding high-dose group (NTP, 1995); BMR = 10% extra risk.	C-42
Table C-20. Summary of BMD modeling results for renal tubule adenoma or carcinoma in male F344 rats exposed to <i>tert</i> -butanol in drinking water for 2 years modeled with administered dose units and including all dose groups; reanalyzed data (Hard et al., 2011; NTP, 1995); BMR = 10% extra risk.....	C-44
Table C-21. Summary of BMD modeling results for renal tubule adenoma or carcinoma in male F344 rats exposed to <i>tert</i> -butanol in drinking water for 2 years modeled with administered dose units and excluding high-dose group; re-analyzed data (Hard et al., 2011; NTP, 1995); BMR = 10% extra risk.....	C-44
Table C-22. Summary of BMD modeling results for renal tubule adenoma or carcinoma in male F344 rats exposed to <i>tert</i> -butanol in drinking water for 2 years modeled with PBPK (<i>tert</i> -butanol, mg/L) dose units and including all dose groups; reanalyzed data (Hard et al., 2011; NTP, 1995); BMR = 10% extra risk.....	C-47
Table C-23. Summary of BMD modeling results for renal tubule adenoma or carcinoma in male F344 rats exposed to <i>tert</i> -butanol in drinking water for 2 years modeled with PBPK (<i>tert</i> -butanol, mg/L) dose units and excluding high-dose group; reanalyzed data (Hard et al., 2011; NTP, 1995); BMR = 10% extra risk.....	C-47
Table C-24. Summary of BMD modeling results for renal tubule adenoma or carcinoma in male F344 rats exposed to <i>tert</i> -butanol in drinking water for 2 years modeled with PBPK (metabolized, mg/hr) dose units and including all dose groups; reanalyzed data (Hard et al., 2011; NTP, 1995); BMR = 10% extra risk.....	C-49
Table C-25. Summary of BMD modeling results for renal tubule adenoma or carcinoma in male F344 rats exposed to <i>tert</i> -butanol in drinking water for 2 years modeled with PBPK (metabolized, mg/hr) dose units and excluding high-dose group; reanalyzed data (Hard et al., 2011; NTP, 1995); BMR = 10% extra risk.....	C-49
Table C-26. Summary of BMD modeling results for thyroid follicular cell adenomas in female B6C3F1 mice exposed to <i>tert</i> -butanol in drinking water for 2 years (NTP, 1995); BMR = 10% extra risk.	C-52

FIGURES

Figure B-1. Biotransformation of <i>tert</i> -butanol in rats and humans.	B-3
Figure B-2. Comparison of the <i>tert</i> -butanol portions of existing MTBE models with <i>tert</i> -butanol blood concentrations from i.v. exposure by Poet et al. 1997.	B-9
Figure B-3. Schematic of the PBPK submodel for <i>tert</i> -butanol in rats.	B-11
Figure B-4. Comparison of the EPA model predictions with measured <i>tert</i> -butanol blood concentrations for i.v., inhalation, and oral gavage exposure to <i>tert</i> -butanol.	B-13
Figure B-5. Comparison of the EPA model predictions with measured amounts of <i>tert</i> -butanol in blood after repeated inhalation exposure to <i>tert</i> -butanol.	B-16
Figure C-1. Plot of mean response by dose, with fitted curve for selected model.	C-4
Figure C-2. Plot of mean response by dose, with fitted curve for selected model.	C-7
Figure C-3. Plot of mean response by dose, with fitted curve for selected model (10% relative deviation).	C-10
Figure C-4. Plot of mean response by dose, with fitted curve for selected model (10% relative deviation).	C-13
Figure C-5. Plot of mean response by dose, with fitted curve for selected model.	C-16
Figure C-6. Plot of mean response by dose, with fitted curve for selected model.	C-20
Figure C-7. Plot of mean response by dose, with fitted curve for selected model; dose shown in mg/m ³	C-24
Figure C-8. Plot of mean response by dose, with fitted curve for selected model; dose shown in mg/m ³	C-27
Figure C-9. Plot of incidence rate by dose, with fitted curve for selected model; dose shown in mg/kg-d.	C-32
Figure C-10. Plot of incidence rate by dose, with fitted curve for selected model; dose shown in mg/kg-d.	C-34
Figure C-11. Plot of incidence rate by dose, with fitted curve for selected model; dose shown in mg/L.	C-36
Figure C-12. Plot of incidence rate by dose, with fitted curve for selected model; dose shown in mg/L.	C-38
Figure C-13. Plot of incidence rate by dose, with fitted curve for selected model; dose shown in mg/hr.	C-40
Figure C-14. Plot of incidence rate by dose, with fitted curve for selected model; dose shown in mg/hr.	C-42
Figure C-15. Plot of incidence rate by dose, with fitted curve for selected model; dose shown in mg/kg-d.	C-45
Figure C-16. Plot of incidence rate by dose, with fitted curve for selected model; dose shown in mg/L.	C-48
Figure C-17. Plot of incidence rate by dose, with fitted curve for selected model; dose shown in mg/hr.	C-50
Figure C-18. Plot of mean response by dose, with fitted curve for selected model.	C-52

ABBREVIATIONS

AIC	Akaike's information criterion
ARCO	ARCO Chemical Company
BMD	benchmark dose
BMDL	benchmark dose lower confidence limit
BMDS	Benchmark Dose Software
BMDU	benchmark dose upper confidence limit
BMR	benchmark response
BW	body weight
CA	chromosomal aberration
CFR	Code of Federal Regulations
CHO	Chinese hamster ovary
CYP450	cytochrome P450
DMSO	dimethyl sulfoxide
DNA	deoxyribonucleic acid
EDTA	ethylenediaminetetraacetic acid
EPA	U.S. Environmental Protection Agency
ETBE	ethyl tert-butyl ether
HBA	2-hydroxyisobutyrate
HL	human leukemia
IC ₅₀	half maximal inhibitory concentration
i.p.	intraperitoneal
i.v.	intravenous
MFO	mixed function oxidase
MPD	2-methyl-1,2-propanediol
MTBE	methyl tert-butyl ether
NADPH	nicotinamide adenine dinucleotide phosphate
NTP	National Toxicology Program
OH	hydroxyl radical
PBPK	physiologically based pharmacokinetic
POD	point of departure
SD	standard deviation
SE	standard error
TWA	time-weighted average

APPENDIX A. OTHER AGENCY AND INTERNATIONAL ASSESSMENTS

A.1. OTHER AGENCY AND INTERNATIONAL ASSESSMENTS

Table A-1. Other Agency and International Assessments.

Organization	Toxicity value
American Conference of Governmental Industrial Hygienists (ACGIH, 2012)	Threshold Limit Value – 100 ppm (303.1493 mg/m ³) time-weighted average (TWA) for an 8-hour workday and a 40-hour work week
National Institute of Occupational Safety and Health (NIOSH, 2007)	Recommended Exposure Limit – 100 ppm (300 mg/m ³) TWA for up to a 10-hour workday and a 40-hour work week
Occupational Safety and Health (OSHA, 2006)	Permissible Exposure Limit for general industry – 100 ppm (300 mg/m ³) TWA for an 8-hour workday
Food and Drug Administration (FDA, 2011a, b)	<i>tert</i> -Butyl alcohol: Indirect food additive that may be safely used in surface lubricants employed in the manufacture of metallic articles that contact food, subject to the provisions of this section (21 Code of Federal Regulations [CFR] 178.3910); substance may be used as a defoaming agent (21 CFR 176.200).

APPENDIX B. INFORMATION IN SUPPORT OF HAZARD IDENTIFICATION AND DOSE-RESPONSE ANALYSIS

B.1. TOXICOKINETICS

There is little information on the absorption, distribution, metabolism, or excretion of *tert*-butyl alcohol (*tert*-butanol) in humans. The studies identified were conducted in conjunction with methyl *tert*-butyl ether (MTBE) and ethyl *tert*-butyl ether (ETBE) because *tert*-butanol is a primary metabolite of these two compounds. Several studies examining some aspect of the toxicokinetic behavior of *tert*-butanol in animals have been identified. Many of the studies were carried out in conjunction with other specific endpoints (e.g., developmental). [ARCO \(1983\)](#) determined that there were no differences in the pharmacokinetics of *tert*-butanol following either oral (i.e., gavage) or inhalation exposure. Although there is some information available after both oral and inhalation exposures, many studies also administered *tert*-butanol via intraperitoneal (i.p.) or intravenous (i.v.) injection. Although these studies do not inform the absorption of *tert*-butanol, they can provide information on distribution, metabolism, and excretion.

B.1.1. Absorption

Extensive *tert*-butanol toxicity testing data submitted by industry to the U.S. Environmental Protection Agency (EPA) under Section 8(e) of the Toxic Substances Control Act and other reporting requirements indicate that *tert*-butanol is rapidly absorbed after oral administration. Very little of the administered dose was excreted in the feces of rats, indicating 99% of the compound was absorbed. Comparable blood levels of *tert*-butanol and its metabolites have been observed after acute oral (350 mg/kg) and inhalation (6,164 mg/m³ for 6 hours) exposures ([ARCO, 1983](#)); however, the absorption rate after inhalation exposure could not be determined because the blood was saturated with radioactivity after 6 hours of a 6,164-mg/m³ exposure. Based on blood concentrations, absorption was found to be complete at 1.5 hours following repeated oral exposure, with an apparent zero-order decline in *tert*-butanol concentration for the majority of the elimination phase, thus indicating that previous exposures did not affect the absorption of *tert*-butanol ([Faulkner et al., 1989](#)).

B.1.2. Distribution

The available animal data suggest that *tert*-butanol is distributed throughout the body following oral, inhalation, and injection exposures ([Poet et al., 1997](#); [Faulkner et al., 1989](#); [ARCO, 1983](#)). [Nihlén et al. \(1995\)](#) determined a partition coefficient for *tert*-butanol using blood from human volunteers. The study was approved by an ethical review board, and informed consent was

obtained from the participants. Their results indicated that *tert*-butanol would rapidly move from the blood into the tissues.

tert-Butanol was found in the kidney, liver, and blood of both sexes of rat following oral exposure, but male rats retained more *tert*-butanol compared with females ([Williams and Borghoff, 2001](#)). Radioactivity was found in the low-molecular-weight protein fraction from the kidney cytosol in male rats but not female rats, indicating that *tert*-butanol or one of its metabolites was bound to α_{2u} -globulin. Further analysis determined that it was *tert*-butanol that was bound and not its metabolite acetone. The majority of *tert*-butanol in the kidney cytosol was eluted as the free compound in both males and females, but a small amount was also found associated with the high-molecular-weight protein fraction in both males and females. [Borghoff et al. \(2001\)](#) found similar results in rats after inhalation exposure. Male rat kidney-to-blood ratios were significantly elevated over female ratios at all dose levels and exposure durations. Although the female *tert*-butanol kidney-to-blood ratio remained similar with both duration and concentration, the male *tert*-butanol kidney-to-blood ratio increased with duration. The liver-to-blood ratios were similar regardless of exposure duration, concentration, or sex. Both of these studies indicate distribution to the liver and kidney with kidney retention of *tert*-butanol in the male rat.

B.1.3. Metabolism

A general metabolic scheme for *tert*-butanol, illustrating the biotransformation in rats and humans, is shown in Figure B–1 below. Urinary metabolites of *tert*-butanol in a human male volunteers who ingested a gelatin capsule containing 5 mg/kg [^{13}C]-*tert*-butanol were reported to be 2-methyl-1,2-propanediol (MPD) and 2-hydroxyisobutyrate ([Bernauer et al., 1998](#)). Minor metabolites of unconjugated *tert*-butanol, *tert*-butanol glucuronides, and traces of the sulfate conjugate also were detected. The study was approved by an ethical review board; however, no information regarding informed consent was reported. In the same study, 2-hydroxyisobutyrate, MPD, and *tert*-butanol sulfate were identified as major metabolites in rats, while acetone, *tert*-butanol, and *tert*-butanol glucuronides were identified as minor metabolites ([Bernauer et al., 1998](#)). [Baker et al. \(1982\)](#) found that *tert*-butanol was a source of acetone, but also may have stimulated acetone production from other sources.

There are no studies that identify specific enzymes responsible for the biotransformation of *tert*-butanol. Using purified enzymes from Sprague-Dawley rats or whole-liver cytosol from Wistar rats, alcohol dehydrogenase had negligible or no activity toward *tert*-butanol ([Videla et al., 1982](#); [Arslanian et al., 1971](#)). Other in vitro studies have implicated the liver microsomal mixed function oxidase (MFO) system, namely cytochrome P-450 (CYP450) ([Cederbaum et al., 1983](#); [Cederbaum and Cohen, 1980](#)). In the first study, incubation of *tert*-butanol at 35 mM with Sprague-Dawley rat liver microsomes and a nicotinamide adenine dinucleotide phosphate- (NADPH) generating system resulted in the production of formaldehyde at a concentration of approximately 25 nmoles/mg protein/30 min. According to study authors, the amount of formaldehyde generated by *tert*-butanol is approximately 30% of the amount of formaldehyde formed during the metabolism of 10 mM

aminopyrene in a similar microsomal system. The rate of formaldehyde generation from *tert*-butanol was increased to about 90 nmol/mg protein/30 min upon addition of azide, which inhibits catalase and thereby prevents the decomposition of hydrogen peroxide (H₂O₂). In other experiments within the same study, there was a major reduction of formaldehyde formation when H₂O₂ was included but NADPH was absent or when the microsomes were boiled prior to incubation. Additionally, the rate of formaldehyde formation in the microsomal oxidizing system was found to be dependent on the concentration of *tert*-butanol, with apparent K_m and V_{max} values of 30 mM and 5.5 nmol/min/mg protein, respectively. The study authors concluded that *tert*-butanol is metabolized to formaldehyde by a mechanism involving oxidation of NADPH, microsomal electron flow, and the generation of hydroxyl-radical (·OH) from H₂O₂, possibly by a Fenton-type or a Haber-Weiss iron-catalyzed reaction involving CYP450, which might serve as the iron chelate (Cederbaum and Cohen, 1980).

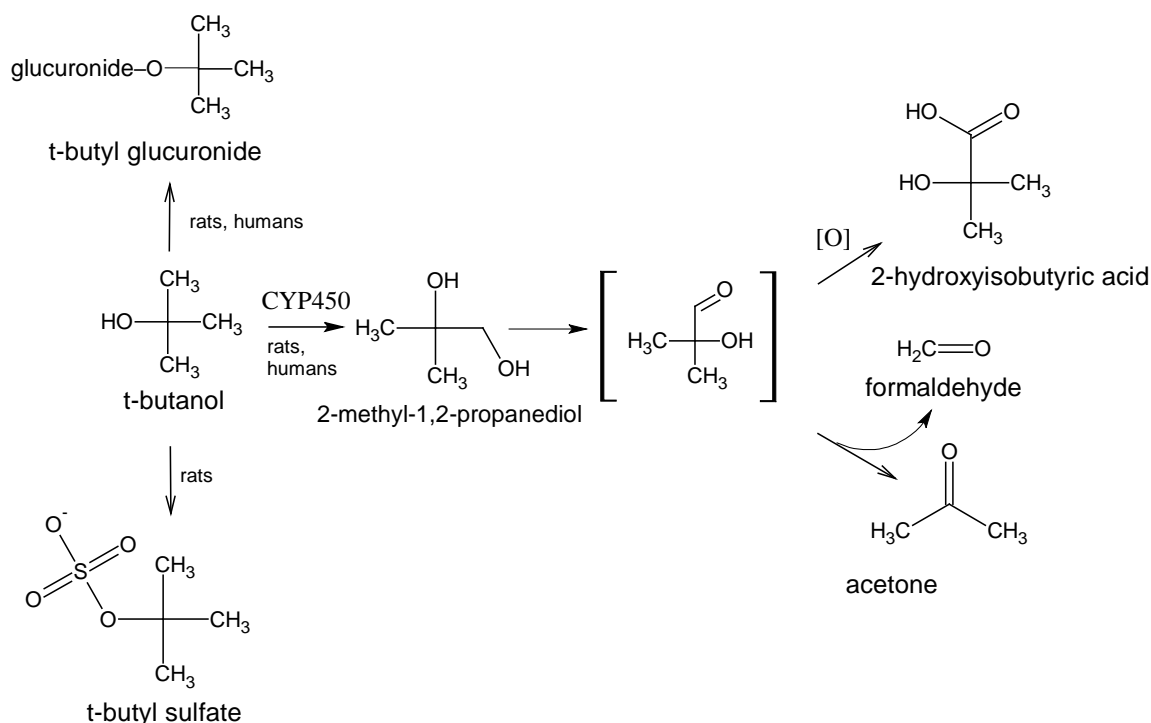
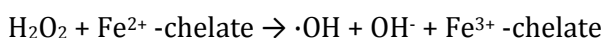


Figure B-1. Biotransformation of *tert*-butanol in rats and humans.

Source: NSF International (2003), ATSDR (1996), Bernauer et al. (1998), Amberg et al. (1999), and Cederbaum and Cohen (1980).

In a follow-up study, *tert*-butanol was oxidized to formaldehyde and acetone by a variety of systems known to generate ·OH radical, including rat liver microsomes or other nonmicrosomal ·OH generating systems (Cederbaum et al., 1983). The nonmicrosomal tests included two chemical systems: (1) the iron-catalyzed oxidation of ascorbic acid (ascorbate-Fe-EDTA

[ethylenediaminetetraacetic acid]) and (2) the Fenton system of chelated ferrous iron and H₂O₂. In both of these Fenton-type systems, H₂O₂ served as a precursor of ·OH. Additionally, a Haber-Weiss enzymatic system involving oxidation of xanthine by xanthine oxidase in the presence of Fe-EDTA was used. In this system, ·OH is thought to be produced by the interaction of H₂O₂ and superoxide (O₂^{·-}). Further experiments demonstrated the involvement of ·OH in either the ascorbate-Fe-EDTA or the xanthine oxidation systems based on inhibition of formaldehyde and acetone production from *tert*-butanol upon addition of ·OH-scavenging agents (e.g., benzoate, mannitol). Some of the experiments in this study of the oxidation of *tert*-butanol by the liver microsomal metabolizing system were similar to those in the previous study except that, in addition to formaldehyde, acetone formation was also measured. Again, these experiments showed the dependence of the microsomal metabolizing system on an NADPH-generating system and the ability of H₂O₂ to enhance, but not replace, the NADPH-generating system. Addition of chelated iron (Fe-EDTA) boosted the microsomal production of formaldehyde and acetone, while ·OH scavenging agents inhibited their production. The study authors noted that neither Fe-EDTA nor ·OH scavenging agents is known to affect the CYP450 catalyzed oxidation of typical MFO substrates such as aminopyrene or aniline. The study also showed that known CYP450 inhibitors, such as metyrapone or SKF-525A, inhibited the production of formaldehyde from aminopyrene but not from *tert*-butanol. Finally, typical inducers of CYP450 and its MFO metabolizing activities, such as phenobarbital or 3-methylcholanthrene, had no effect on the extent of microsomal metabolism of *tert*-butanol to formaldehyde and acetone. According to the study authors, the oxidation of *tert*-butanol appears to be mediated by ·OH (possibly via H₂O₂), which can be produced by any of the tested systems by a Fenton-type reaction as follows:



According to this reaction, reduction of ferric iron (Fe³⁺) to ferrous iron (Fe²⁺) is required for continuous activity. The study authors concluded that the nature of the iron and the pathway of iron reduction within the microsomes remain to be elucidated even though an NADPH-dependent electron transfer or O₂^{·-} might be involved ([Cederbaum et al., 1983](#)).

B.1.4. Excretion

Human data on the excretion of *tert*-butanol comes from studies of MTBE and ETBE ([Nihlén et al., 1998a, b](#)). Eight or ten male human volunteers were exposed to 5, 25, or 50 ppm MTBE or ETBE by inhalation during 2 hours of light exercise. The half-life of *tert*-butanol in urine following MTBE exposure was 8.1 ± 2.0 hours (average of the 25- and 50-ppm MTBE doses); the half-life of *tert*-butanol in urine following ETBE exposure was 7.9 ± 2.7 hours (average of 25- and 50-ppm ETBE doses). The renal clearance rate of *tert*-butanol was 0.67 ± 0.11 mL/hr·kg with MTBE exposure (average of 25- and 50-ppm MTBE doses); the renal clearance rate was 0.80 ± 0.34 mL/hr·kg with ETBE exposure (average of 25- and 50-ppm ETBE doses).

[Amberg et al. \(2000\)](#) exposed six volunteers (three males and three females, 28 ± 2 years old) to 18.8 and 170 mg/m³ ETBE. Each exposure lasted 4 hours, and the two concentrations were administered to the same volunteers 4 weeks apart. Urine was collected at 6-hour intervals for 72 hours following exposure. *tert*-Butanol and two metabolites of *tert*-butanol, 2-hydroxyisobutyrate (HBA) and MPD, also were identified in urine. At an ETBE level of 170 mg/m³, *tert*-butanol displayed a half-life of 9.8 ± 1.4 hours. At the low-exposure ETBE concentration, the *tert*-butanol half-life was 8.2 ± 2.2 hours. The predominant urinary metabolite identified was HBA, excreted in urine at 5–10 times the amount of MPD and 12–18 times the amount of *tert*-butanol (note: urine samples had been treated with acid before analysis to cleave conjugates). HBA in urine showed a broad maximum at 12–30 hours after exposure to both concentrations, with a slow decline thereafter. MPD in urine peaked at 12 and 18 hours after exposure to 170 and 18.8 mg/m³ ETBE, respectively, while *tert*-butanol peaked at 6 hours after both concentrations.

[Amberg et al. \(2000\)](#) exposed F344 NH rats to 18.8 and 170 mg/m³ ETBE. Urine was collected for 72 hours following exposure. Similar to humans, rats excreted mostly HBA in urine, followed by MPD and *tert*-butanol. The half-life for *tert*-butanol in rat urine was 4.6 ± 1.4 hours at ETBE levels of 170 mg/m³, but half-life could not be calculated at the ETBE concentration of 18.8 mg/m³. Corresponding half-lives were 2.6 ± 0.5 and 4.0 ± 0.9 hours for MPD and 3.0 ± 1.0 and 4.7 ± 2.6 hours for HBA. In Sprague-Dawley rats treated with radiolabeled *tert*-butanol by gavage at 1, 30, or 500 mg/kg, a fairly constant fraction of the administered radioactivity (23–33%) was recovered in the urine at 24 hours postdosing. However, only 9% of a 1500-mg/kg administered dose was recovered in urine, suggesting that the urinary route of elimination is saturated following this dose ([ARCO, 1983](#)).

B.1.5. Physiologically Based Pharmacokinetic Models

There have been no physiologically based pharmacokinetic (PBPK) models developed specifically for administration of *tert*-butanol. The majority studied *tert*-butanol as the primary metabolite after oral or inhalation exposure to MTBE or ETBE. The most recent models for MTBE oral and inhalation exposure include a component for the binding of *tert*-butanol to α_{2u} -globulin ([Borghoff et al., 2010](#); [Leavens and Borghoff, 2009](#)).

[Faulkner and Hussain \(1989\)](#) used a one-compartment open model with Michaelis-Menten elimination kinetics to fit *tert*-butanol blood concentrations obtained from C57BL/6J mice given i.p. injections of 5, 10, or 20 mmol/kg *tert*-butanol. Elimination was indistinguishable from first-order kinetics in the range of concentrations studied. An increase in V_{\max} and decrease in apparent volume of distribution with dose are consistent with this model and suggest the existence of parallel elimination processes.

[Borghoff et al. \(1996\)](#) developed a PBPK model for MTBE and its metabolite *tert*-butanol in rats. Doses and blood levels were taken from several published studies. The initial model included a tissue-specific five-compartment model using blood, liver, kidney, muscle, and fat with liver

metabolism rate constants. The model was able to predict the accumulation of *tert*-butanol in blood, but not its clearance. A two-compartment model was better at predicting *tert*-butanol blood levels, however, the volume of the total body water had to be changed to obtain an adequate fit, suggesting dose-dependent changes in the kinetics of *tert*-butanol. Overall, evaluation of the *tert*-butanol models suggests that the clearance of *tert*-butanol from the blood of rats after exposure to MTBE involves processes beyond metabolic elimination.

[Nihlén and Johanson \(1999\)](#) developed a PBPK model for evaluation of inhalation exposure in humans to the gasoline additive ETBE. Model compartments for ETBE included lungs (with arterial blood), liver, fat, rapidly perfused tissues, resting muscles, and working muscles. The same set of compartments and an additional urinary excretion compartment were used for the metabolite, *tert*-butanol. First-order metabolism was assumed in the model, and tissue/blood partition coefficients were determined by in vitro methods ([Nihlén et al., 1995](#)). Estimates of individual metabolite parameters of eight subjects were obtained by fitting the PBPK model to experimental data from humans (5, 25, or 50 ppm ETBE; 2-hour exposure) ([Nihlén et al., 1998a](#)). This model was applied primarily to predict levels of the biomarkers ETBE and *tert*-butanol in blood, urine, and exhaled air after various scenarios, such as prolonged exposure, fluctuating exposure, and exposure during physical activity ([Nihlén and Johanson, 1999](#)).

[Rao and Ginsberg \(1997\)](#) developed a PBPK model for MTBE and its principal metabolite, *tert*-butanol, based on the [Borghoff et al. \(1996\)](#) model. The modified model included a skin compartment to simulate dermal absorption of MTBE during bathing or showering. A brain compartment was added as a target organ for MTBE-induced neurological responses. MTBE metabolism to *tert*-butanol was assumed to occur in the liver through two saturable pathways. The *tert*-butanol portion of the model included further metabolism of *tert*-butanol in the liver, exhalation in the lungs, and renal excretion (in the human model only). The model was validated against published human and rat data and was used to help determine the contribution of *tert*-butanol in the acute central nervous system effects seen after MTBE dosing.

The [Rao and Ginsberg \(1997\)](#) model used peak concentrations of MTBE and *tert*-butanol in the blood and brain for interspecies, route-to-route, and low/high-dose extrapolations. The MTBE/*tert*-butanol PBPK model was adapted to humans by adjusting physiology according to literature values, incorporating the blood/air partition coefficient for humans reported by [Johanson et al. \(1995\)](#), and allometrically scaling the metabolic rate based on body weight. A renal elimination component was added to account for the small percentage of MTBE disposition that occurs in humans via urinary excretion of *tert*-butanol. *tert*-Butanol concentrations in human blood during and after MTBE exposure (25 or 50 ppm for 2 hours) were accurately predicted by the human model ([Johanson et al., 1995](#)).

[Kim et al. \(2007\)](#) expanded the [Borghoff et al. \(1996\)](#) model to develop a multi-exposure route model for MTBE and its primary metabolite, *tert*-butanol, in humans. The significant features and advantages of the [Kim et al. \(2007\)](#) model are that parameters used for quantifying the

pharmacokinetic behavior of MTBE and *tert*-butanol are calibrated using time-series measurements from controlled-exposure experiments in humans as reported by Prah et al. (2004). MTBE partition coefficient values described in the Licata et al. (2001) model and skin compartment parameters from the Rao and Ginsberg (1997) model were incorporated. The PBPK model for MTBE consists of nine primary compartments representing the lungs, skin, fat, kidney, stomach, intestine, liver, rapidly perfused tissue, and slowly perfused tissue. The *tert*-butanol model consists of three compartments representing blood, liver, and other tissue.

Leavens and Borghoff (2009) developed a PBPK model for inhalation exposures in male and female rats that expanded on Borghoff et al. (1996) and Rao and Ginsberg (1997) to include the sex-specific effects of MTBE binding to α_{2u} -globulin, a protein unique to male rats, and to describe the induction of *tert*-butanol metabolism after repeated exposures. Although the primary purpose of the model was to estimate MTBE and *tert*-butanol tissue concentrations after MTBE exposure, the model was also parameterized to include inhalation uptake of *tert*-butanol. The *tert*-butanol portion of the model was calibrated using data from rat exposures to *tert*-butanol as well as MTBE. Model compartments included blood, brain, fat, gastrointestinal tissues, kidney, liver, poorly perfused tissues (blood flow of <100 mL/min/100 g of tissue: bone, muscle, skin, fat), and rapidly perfused tissues.

Distribution of MTBE and *tert*-butanol was assumed to be perfusion (i.e., blood-flow) limited. This model used the same assumptions as Borghoff et al. (1996) regarding MTBE metabolism and kinetics, and assumed that *tert*-butanol was metabolized only in the liver through one low-affinity pathway and excreted through urine. The model described binding of MTBE or *tert*-butanol with α_{2u} -globulin in the kidney, due to the high concentration of α_{2u} -globulin in the kidney. As chemicals bind to α_{2u} -globulin, the rate of hydrolysis of the protein decreases and causes accumulation in the kidney; however, there is no evidence that binding of α_{2u} -globulin affects its synthesis, secretion, or circulating concentrations [Borghoff et al. (1990) as cited in Leavens and Borghoff (2009)]. Equations describing this phenomenon were included in the model for male rats only to account for the effects of the binding with α_{2u} -globulin on metabolism of MTBE and *tert*-butanol. Partition coefficient values in the model that differed from those published in previous PBPK models included poorly perfused tissues:blood and kidney:blood values. The kidney:blood value was based on calculated kidney:blood concentrations in female rats only because of the lack of α_{2u} -globulin-associated effects in female rats. The deposition of *tert*-butanol during inhalation in the nasal cavity and upper airways was reflected in the high blood:air partition coefficient for *tert*-butanol, and the ability of *tert*-butanol to induce its own metabolism after chronic exposure was also taken into account. No differences in the induction of metabolism were reported between males and females. The model simulated concentrations of MTBE and *tert*-butanol in the brain, liver, and kidney of male and female rats following inhalation exposure at concentrations of 100, 400, 1,750, or 3,000 ppm MTBE, and compared them to measured concentrations of MTBE and *tert*-butanol from rats exposed at those levels.

Concentrations of MTBE and *tert*-butanol in the brain and liver were similar in male and female rats during exposure and postexposure, but the concentrations of the chemicals in the kidney were significantly different in male rats when compared with female rats. The additional parameter accounting for $\alpha_2\mu$ -globulin protein-binding in this PBPK model more accurately reflects the metabolism of both MTBE and *tert*-butanol in male rat kidneys over time compared with other PBPK models. The model highlights that binding can stimulate increased renal effects in male rats after exposure to MTBE and *tert*-butanol. The assumptions made to reflect *tert*-butanol metabolism induction and deposition in the nasal cavity and upper airways generally were supported by measured data from rats exposed to 250, 450, or 1,750 ppm *tert*-butanol as evidenced by the fact that the model was within one standard deviation of the mean concentrations for most data points. However, the model overpredicted the concentration of *tert*-butanol in the brain, liver, and kidney of male rats after repeated exposures.

[Borghoff et al. \(2010\)](#) modified the PBPK model of [Leavens and Borghoff \(2009\)](#) by adding oral gavage and drinking water exposure components. This was done to compare different dose metrics to the toxicity observed across different studies. The [Borghoff et al. \(2010\)](#) model assumed first-order uptake of MTBE absorption from the gut, with 100% of the MTBE dose absorbed for both drinking water and oral gavage exposures. They conducted a series of pharmacokinetic studies comparing the effects of different rat strains and different dosing vehicles on the blood concentration-time profiles of MTBE and *tert*-butanol following MTBE exposure. The effects of exposure to MTBE via drinking water, oral gavage, and inhalation routes over 7 and 91 days on male and female rats were modeled and compared with measured data collected from F344 rats (exposed 28 days) and Wistar Han rats (exposed 14 and 93 days).

The model predicted the blood concentrations of *tert*-butanol that were observed after 250 or 1,000 mg/kg-day administration of MTBE in males and females, as well as the blood concentrations of MTBE after 1,000 mg/kg-day, but was not able to predict peak concentrations of MTBE after 250 mg/kg-day in males or females using either olive oil or 2% Emulphor as vehicles. When comparing strains, the blood concentrations were similar across strain and sex, except in female Sprague-Dawley rats administered 1,000 mg/kg-day MTBE. The female Sprague-Dawley rats had a significantly (*p*-value not specified) higher blood concentration of both MTBE and *tert*-butanol compared with the F344 and the Wistar Han females. However, the study authors considered this an outlier and still considered the metabolic patterns similar. The model overpredicted the amount of MTBE in the male rat kidney, but it accurately predicted the level of *tert*-butanol in the male rat kidney at all exposures tested. The model did not accurately predict the kidney concentrations of *tert*-butanol in the female kidney after exposure to MTBE via drinking water, but the study authors attributed the inaccuracies to the study design as opposed to the model formulation. All of the *tert*-butanol entering the submodel comes from MTBE metabolism in the liver, and the model does not include a separate oral intake of *tert*-butanol.

B.2. PBPK MODEL EVALUATION SUMMARY

B.2.1. Evaluation of Existing *tert*-Butanol Submodels

The [Blancato et al. \(2007\)](#) and [Leavens and Borghoff \(2009\)](#) PBPK models for MTBE were evaluated by comparing predictions from the *tert*-butanol portions of the models with the *tert*-butanol i.v. data of [Poet et al. \(1997\)](#) (see Figure B-2). Neither model adequately represented the *tert*-butanol blood concentrations. Modifications of model assumptions for alveolar ventilation, explicit pulmonary compartments, and induction of metabolism of *tert*-butanol did not significantly improve model fits to the data. Attempts to reoptimize model parameters in the *tert*-butanol submodels of [Blancato et al. \(2007\)](#) and [Leavens and Borghoff \(2009\)](#) to match blood concentrations from the i.v. dosing study were unsuccessful.

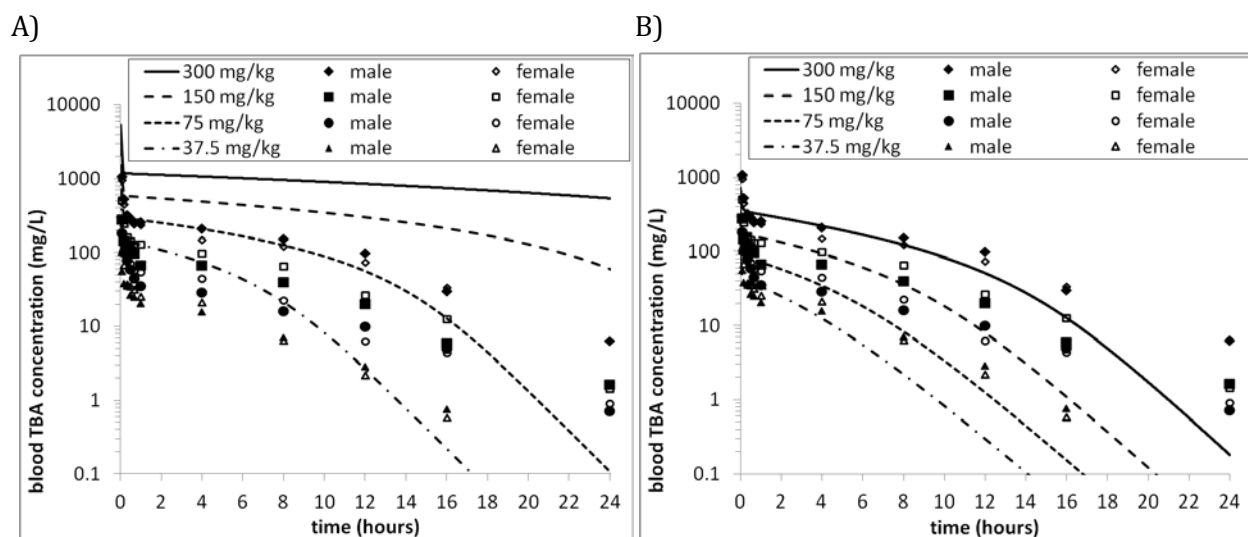


Figure B-2. Comparison of the *tert*-butanol portions of existing MTBE models with *tert*-butanol blood concentrations from i.v. exposure by Poet et al. 1997.

Neither the a) [Blancato et al. \(2007\)](#) nor the b) [Leavens and Borghoff \(2009\)](#) model adequately represents the measured *tert*-butanol blood concentrations.

The PBPK submodel for *tert*-butanol in rats was developed in acslX (Advanced Continuous Simulation Language, Aegis, Inc., Huntsville, Alabama) by adapting information from the many PBPK models that were developed in rats and humans for the structurally related substance, MTBE, and its metabolite *tert*-butanol ([Borghoff et al., 2010](#); [Leavens and Borghoff, 2009](#); [Blancato et al., 2007](#); [Kim et al., 2007](#); [Rao and Ginsberg, 1997](#); [Borghoff et al., 1996](#)). A brief description comparing the [Blancato et al. \(2007\)](#) and ([Leavens and Borghoff, 2009](#)) models is given, followed by an evaluation of the MTBE models and the assumptions adopted from MTBE models or modified in the *tert*-butanol model.

The [Blancato et al. \(2007\)](#) model is an update of the earlier [Rao and Ginsberg \(1997\)](#) model, and the [Leavens and Borghoff \(2009\)](#) model is an update of the [Borghoff et al. \(1996\)](#) model. Both the [Blancato et al. \(2007\)](#) and [Leavens and Borghoff \(2009\)](#) models are flow-limited models that predict amounts and concentrations of MTBE and its metabolite *tert*-butanol in blood and six tissue compartments: liver, kidney, fat, brain, and rapidly and slowly perfused tissues. These tissue compartments are linked through blood flow, following an anatomically accurate, typical, physiologically based description ([Andersen, 1991](#)). The parent (MTBE) and metabolite (*tert*-butanol) models are interlinked by the metabolism of MTBE to *tert*-butanol in the liver. Routes of exposure included in the models are oral and inhalation for MTBE; [Leavens and Borghoff \(2009\)](#) included inhalation exposure to *tert*-butanol. Oral doses are assumed to be 100% bioavailable and 100% absorbed from the gastrointestinal tract represented with a first-order rate constant. Following inhalation of MTBE or *tert*-butanol, the chemical is assumed to directly enter the systemic blood supply, and the respiratory tract is assumed to be at a pseudo-steady state. Metabolism of MTBE by CYP450s to formaldehyde and *tert*-butanol in the liver is described with two Michaelis-Menten equations representing high- and low-affinity enzymes. *tert*-Butanol is either conjugated with glucuronide or sulfate or further metabolized to acetone through MPD and HBA; both of these processes are described by a single Michaelis-Menten equation in the models. All of these model assumptions are valid for *tert*-butanol and were applied to the EPA-developed *tert*-butanol PBPK model, except for the separate brain compartment. The brain compartment was lumped with other richly perfused tissues in the EPA *tert*-butanol PBPK model.

In addition to differences in parameter values between the [Blancato et al. \(2007\)](#) and the [Leavens and Borghoff \(2009\)](#) models, there were three differences in the model structure: (1) the alveolar ventilation was reduced during exposure, (2) the rate of *tert*-butanol metabolism increased over time due to induction of CYP enzymes, and (3) binding of MTBE and *tert*-butanol to α_{2u} -globulin was simulated in the kidney of male rats. The [Blancato et al. \(2007\)](#) model was configured through EPA's PBPK modeling framework, ERDEM (Exposure-Related Dose Estimating Model), which includes explicit pulmonary compartments. The modeling assumptions related to alveolar ventilation, explicit pulmonary compartments, and induction of metabolism of *tert*-butanol are discussed in the model evaluation section.

MTBE and *tert*-butanol binding to α_{2u} -globulin in the kidneys of male rats were incorporated in the PBPK model of MTBE by [Leavens and Borghoff \(2009\)](#). Binding to α_{2u} -globulin is one hypothesized MOA for the observed kidney effects in MTBE-exposed animals. For a detailed description of the role of α_{2u} -globulin and other MOAs in kidney effects, see the kidney MOA section of this document (see Section 1.1.1). Binding of MTBE to α_{2u} -globulin was applied to sex differences in kidney concentrations of MTBE and *tert*-butanol in the [Leavens and Borghoff \(2009\)](#) model, but acceptable estimates of MTBE and *tert*-butanol pharmacokinetics in the blood are predicted in other models that did not consider α_{2u} -globulin binding. Given the uncertainty of *tert*-butanol binding to α_{2u} -globulin, it was not included in the *tert*-butanol PBPK submodel.

B.2.2. Modification of Existing *tert*-Butanol Submodels

To account for the *tert*-butanol blood concentrations after i.v. *tert*-butanol exposure, the model was modified by adding a pathway for reversible sequestration of *tert*-butanol in the blood. This could represent binding of *tert*-butanol to proteins in blood (see Figure B-3). The JPEC PK studies showed that approximately 60% of the radiolabel in whole blood is in the plasma, providing some limited evidence for association of *tert*-butanol with components in blood. The PBPK model represented the rate of change in the amount of *tert*-butanol in the sequestered blood compartment (A_{blood2}) with the following equation where K_{ON} is the binding rate constant, CV is the free *tert*-butanol concentration in blood, K_{OFF} is the unbinding rate constant, and C_{blood2} is the concentration of *tert*-butanol bound in blood (equal to $A_{\text{blood2}}/V_{\text{blood}}$).

$$dA_{\text{blood2}}/dt = K_{\text{ON}} \cdot CV - K_{\text{OFF}} \cdot C_{\text{blood2}}$$

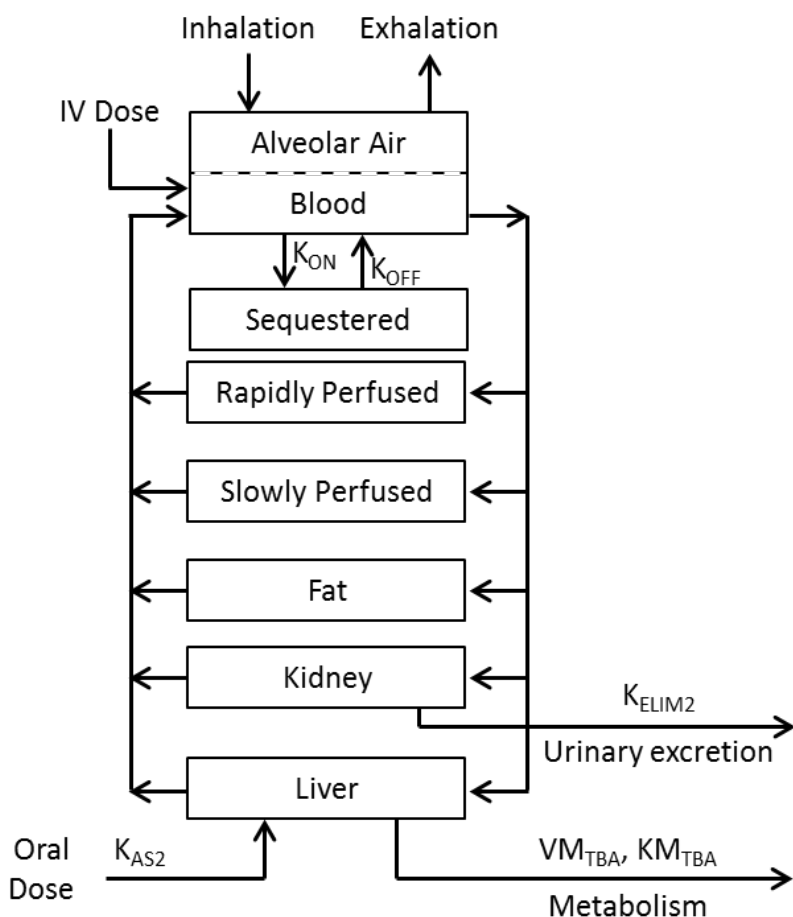


Figure B-3. Schematic of the PBPK submodel for *tert*-butanol in rats.

Exposure can be via multiple routes including inhalation, oral, or i.v. dosing. Metabolism of *tert*-butanol occurs in the liver and is described by Michaelis-Menten equations with one pathway for *tert*-butanol. *tert*-Butanol is cleared via exhalation and *tert*-butanol is additionally cleared via urinary excretion. See Table B-1 for definitions of parameter abbreviations.

Table B-1. PBPK model physiologic parameters and partition coefficients.

Body weight and organ volumes as fraction of body weight		
Body Weight (kg)	0.25	(Brown et al., 1977)
Body fraction that is blood perfused (Fperf)	0.8995	(Brown et al., 1977)
Liver	0.034	(Brown et al., 1977)
Kidney	0.007	(Brown et al., 1977)
Fat	0.07	(Brown et al., 1977)
Rapidly perfused	0.04	(Brown et al., 1977)
Slowly perfused	0.7485 ^a	
Blood	0.074	(Brown et al., 1977)
Cardiac output and organ blood flows as fraction of cardiac output		
Cardiac output (L/hr)	5.38	(Brown et al., 1977) ^b
Alveolar ventilation (L/hr)	5.38	(Brown et al., 1977) ^c
Liver	0.174	(Brown et al., 1977) ^d
Kidney	0.141	(Brown et al., 1977)
Fat	0.07	(Brown et al., 1977)
Rapidly perfused	0.279 ^e	
Slowly perfused	0.336	(Brown et al., 1977)
Partition coefficients for <i>tert</i> -butanol		
Blood:air	481	(Borghoff et al., 1996)
Liver:blood	0.83	(Borghoff et al., 1996)
Fat:blood	0.4	(Borghoff et al., 1996)
Rapidly perfused:blood	0.83	(Borghoff et al., 1996)
Slowly perfused:blood	1.0	(Borghoff et al., 1996)
Kidney:blood	0.83	(Borghoff et al., 1996)

^a Fperf – Σ {other compartments}^b $15.2 \cdot BW^{0.75}$ (bw = body weight)^c Alveolar ventilation is set equal to cardiac output^d Sum of liver and gastrointestinal blood flows^e $1 - \Sigma$ {all other compartments}.

The physiologic parameter values obtained from the literature are shown in Table B-1 ([Brown et al., 1977](#)). *tert*-Butanol partition coefficients were obtained from literature in which they were determined by the ratios of measured tissue:air and blood:air partition coefficients ([Borghoff et al., 1996](#)). The parameters describing rate constants of metabolism and elimination of *tert*-butanol were obtained from the literature ([Blancato et al., 2007](#)) and kept fixed because these have been optimized to *tert*-butanol blood concentrations measured after MTBE exposure, which is also metabolized to *tert*-butanol. The parameters describing *tert*-butanol absorption and *tert*-butanol sequestration in blood were estimated by optimizing the model to the blood *tert*-butanol time-course data for rats exposed via i.v., inhalation, and oral routes ([Leavens and Borghoff, 2009](#); [Poet et al., 1997](#); [ARCO, 1983](#)). The model parameters were estimated with the acslX

optimization routine to minimize the log-likelihood function of estimated and measured *tert*-butanol concentrations. The Nedler-Mead algorithm was used with heteroscedasticity allowed to vary between 0 and 2. The predictions of the model with optimized parameters have a much improved fit to the *tert*-butanol blood concentrations after *tert*-butanol i.v., as shown in panel A of Figure B-4. Additionally, the model adequately estimated the *tert*-butanol blood concentrations after inhalation and oral gavage exposures. The optimized parameter values are shown in Table B-2. The [ARCO \(1983\)](#) study measured *tert*-butanol in plasma only, unlike the [Poet et al. \(1997\)](#) and [Leavens and Borghoff \(2009\)](#) studies that measured *tert*-butanol in whole blood. Based on the measurements of plasma and whole blood by JPEC 2008, the concentration of *tert*-butanol in plasma is approximately 60% of the concentration in whole blood. The *tert*-butanol plasma concentrations measured by ARCO were increased (divided by 60%) to the expected concentration in whole blood for comparison with the PBPK model.

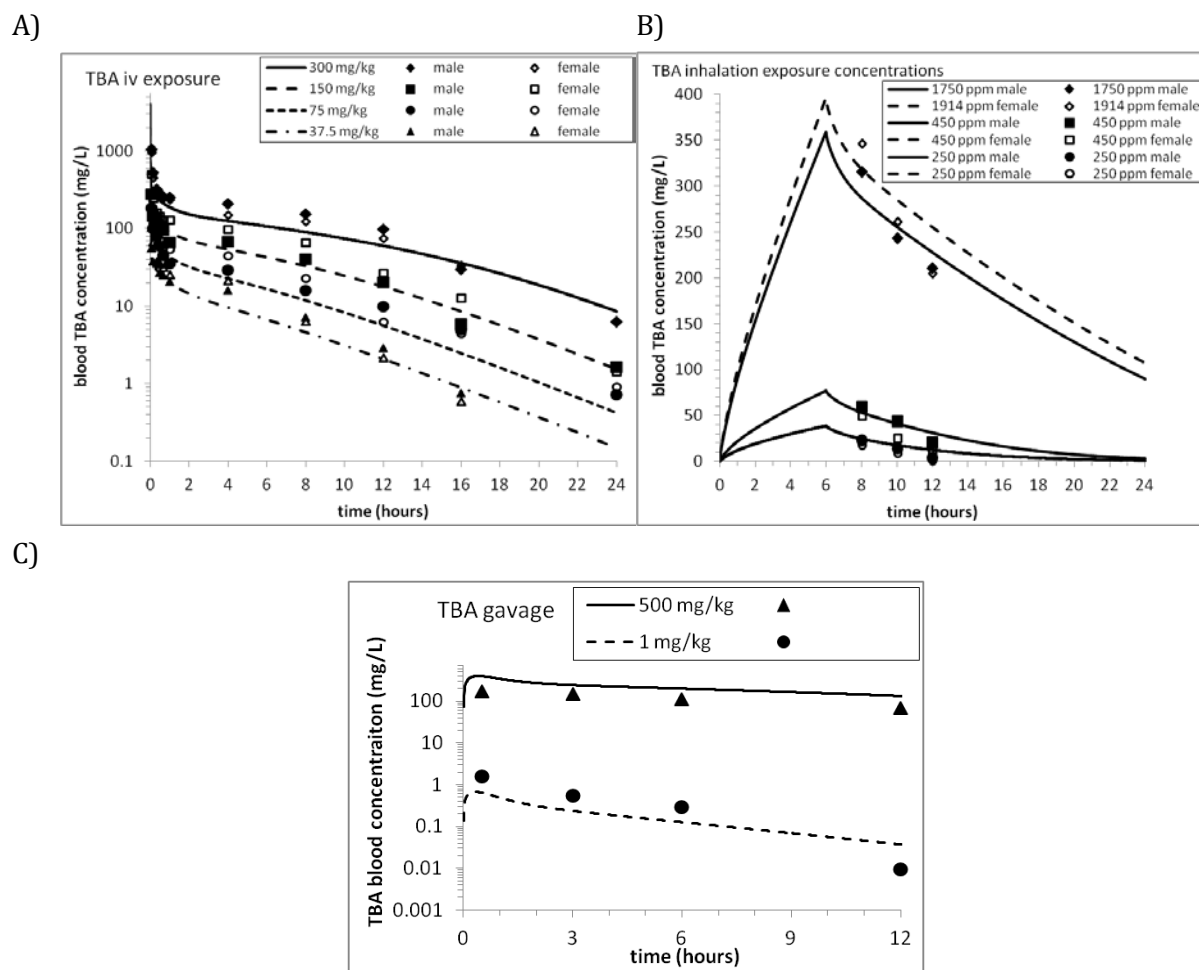


Figure B-4. Comparison of the EPA model predictions with measured *tert*-butanol blood concentrations for i.v., inhalation, and oral gavage exposure to *tert*-butanol.

A) i.v. data from [Poet et al. \(1997\)](#); B) inhalation data from [Leavens and Borghoff \(2009\)](#); and C) oral gavage data from [ARCO \(1983\)](#) with the optimized parameter values as shown in Table B-2.

Table B-2. Rate constants for *tert*-butanol determined by optimization of the model with experimental data.

Parameter	Value	Source or Reference
Metabolism (VM_{TBA} ; mg/kg-hr) ^a	8.0	Blancato et al. (2007)
Metabolism (KM_{TBA} ; mg/L)	28.8	Blancato et al. (2007)
Urinary elimination (K_{ELIM2} ; 1/hr)	0.5	Blancato et al. (2007)
TBA sequestration rate constant (K_{ON} ; L/hr)	0.148	Optimized
TBA unsequestration rate constant (K_{OFF} ; L/hr)	0.0134	Optimized
Absorption from gastrointestinal tract (K_{AS2} ; 1/hr)	0.5	Optimized

^a scaled by $BW^{0.7}$ ($0.25^{0.7} = 0.379$), bw = body weight.

Induction of *tert*-butanol-metabolizing enzymes was included in the [Leavens and Borghoff \(2009\)](#) model of MTBE based on their study of rats exposed for 8 days to *tert*-butanol via inhalation. The enzyme induction equation and parameters developed in the [Leavens and Borghoff \(2009\)](#) model that were applied to the *tert*-butanol submodel are as follows.

$$V_{\max \text{ } tert\text{-butanol IND}} = V_{\max \text{ } tert\text{-butanol}} * IND_{\max}(1 - \exp(-K_{IND} * t))$$

$V_{\max \text{ } tert\text{-butanol IND}}$ is the maximum metabolic rate after accounting for enzyme induction, $V_{\max \text{ } tert\text{-butanol}}$ is the metabolism rate constant from Table B-2 for both *tert*-butanol pathways, and IND_{\max} is the maximum percent increase in $V_{\max \text{ } tert\text{-butanol}}$ (124.9). K_{IND} is the rate constant for enzyme induction (0.3977/day). The increased *tert*-butanol metabolism better estimates the measured *tert*-butanol blood concentrations as can be seen in the comparison of the model predictions and experimental measurements shown in Figure B-5. The model better predicted blood concentrations in female rats than male rats. The male rats had lower *tert*-butanol blood concentrations after repeated exposures compared with female rats, and this difference could indicate greater induction of *tert*-butanol metabolism or other physiologic changes such as ventilation or urinary excretion in males. The current data for *tert*-butanol metabolism do not provide sufficient information for resolving this difference between male and female rats.

B.2.3. Summary of the PBPK model for *tert*-butanol

A PBPK model for *tert*-butanol was developed by adapting previous models for MTBE and *tert*-butanol ([Blancato et al. \(2007\)](#); [Leavens and Borghoff \(2009\)](#)). Published *tert*-butanol models (or sub-models) do not adequately represent the *tert*-butanol blood concentrations measured in the i.v. study (Poet et al. 1997). The addition of a sequestered blood compartment for *tert*-butanol substantially improved the model fit. The alternative modification of changing to diffusion-limited distribution between blood and tissues also improved the model fit, but was considered less biologically plausible. Physiological parameters and partition coefficients were obtained from

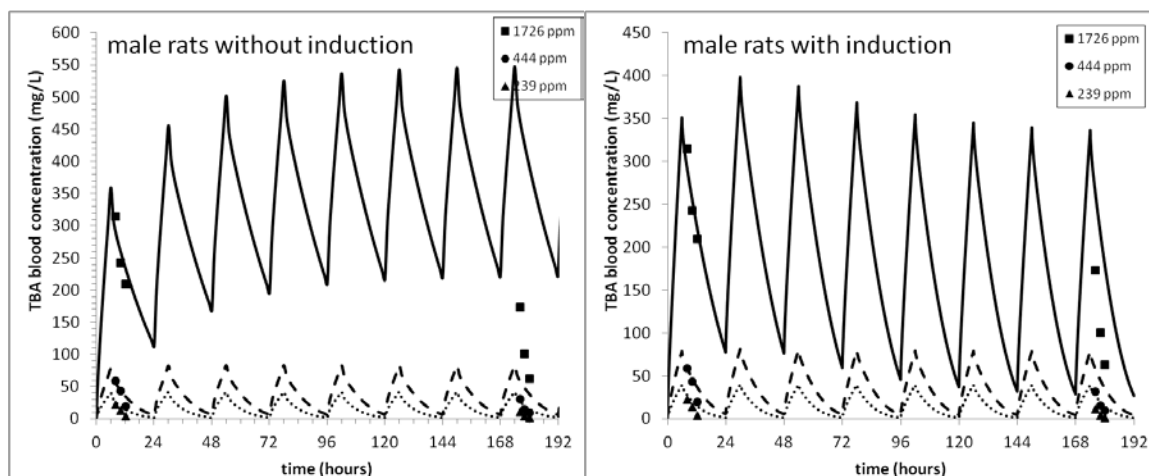
published measurements. The rate constants for tert-butanol metabolism and elimination were from a published PBPK model of MTBE with a tert-butanol subcompartment ([Blancato et al. \(2007\)](#)). Additional model parameters were estimated by calibrating to data sets for i.v., oral and inhalation exposures as well as repeated dosing studies for TBA. Overall, the model produced acceptable fits to multiple rat time-course datasets of TBA blood levels following either inhalation or oral gavage exposures.

B.2.4. tert-Butanol Model Application

The PBPK model as described above was applied to toxicity studies to predict *tert*-butanol blood concentrations (the preferred internal dose metric). For simulation studies where *tert*-butanol was administered in drinking water, the consumption was modeled as episodic, based on the pattern of drinking observed in rats ([Spiteri, 1982](#)).

B.2.5. PBPK Model Code

The PBPK acslX model code is made available electronically through EPA's Health and Environmental Research Online (HERO) database. All model files may be downloaded in a zipped workspace from HERO (U.S. EPA, 201#, HEROID##).



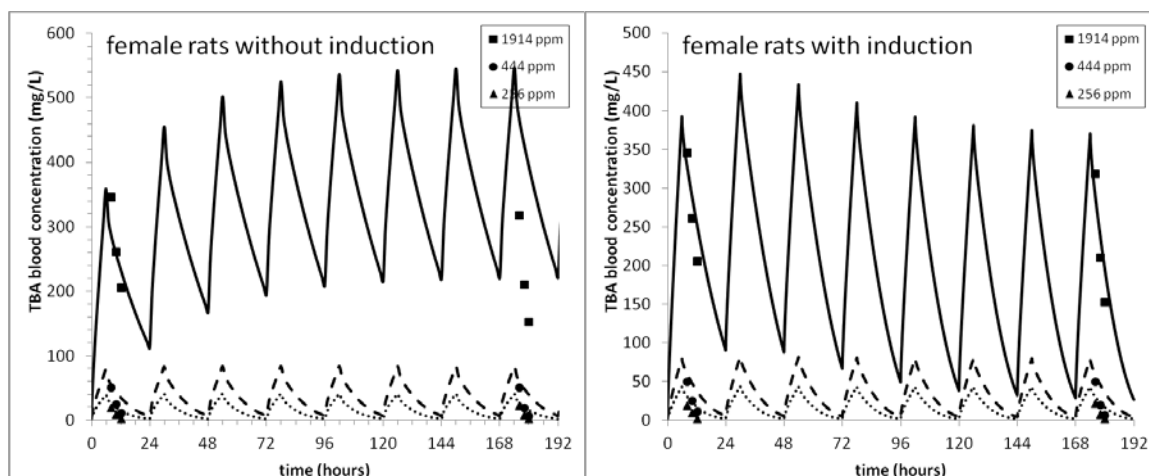


Figure B-5. Comparison of the EPA model predictions with measured amounts of *tert*-butanol in blood after repeated inhalation exposure to *tert*-butanol.

Male rats were exposed to 239, 444, or 1726 ppm and female rats were exposed to 256, 444, or 1914 ppm *tert*-butanol for up to 8 consecutive days ([Borghoff et al., 2001](#)). *tert*-Butanol blood concentrations are better predicted by the model after 8 days of exposure with enzyme induction (right panels) compared to without enzyme induction (left panels).

B.3. OTHER PERTINENT TOXICITY INFORMATION

B.3.1. Genotoxicity

The genotoxic potential of *tert*-butanol has been studied using a variety of genotoxicity assays, including bacterial reverse mutation assays, gene mutation assays, chromosomal aberrations, sister chromatid exchanges, micronucleus formation, and DNA strand breaks and adducts. The available genotoxicity data for *tert*-butanol are discussed below, and the summary of the data is provided in Table B-3.

B.3.1.1. Bacterial Systems

The mutagenic potential of *tert*-butanol has been tested by [Zeiger et al. \(1987\)](#) using different *Salmonella typhimurium* strains both in the presence and absence of S9 metabolic activation. The preincubation assay protocol was followed. *Salmonella* strains TA98, TA100, TA1535, TA1537, and TA1538 were exposed to five concentrations (100, 333, 1,000, 3,333, or 10,000 µg/plate) and tested in triplicate. No mutations were observed in any of the strains tested, either in the presence or absence of S9 metabolic activation.

Conflicting results have been obtained with *tert*-butanol-induced mutagenicity in strain TA102, a strain that is sensitive to damage at A-T sites inducible by oxidants and other mutagens and is excision-repair proficient. In a study by [Williams-Hill et al. \(1999\)](#), *tert*-butanol induced an

increase in the number of revertants in the first three concentrations with S9 activation in a dose-response manner. The number of revertants decreased in the last two concentrations. No discussion was provided as to why the revertants decreased at higher concentrations. The results of this study indicated that tester strain TA102 may be a more sensitive strain for monitoring *tert*-butanol levels ([Williams-Hill et al., 1999](#)). However, in another study by [Mcgregor et al. \(2005\)](#), experiments were conducted on *Salmonella* strain TA102 in two different laboratories using similar protocols. *tert*-Butanol was dissolved in dimethyl sulfoxide (DMSO) or distilled water and tested both in the presence and absence of S9 metabolic activation. No statistically significant increase in mutants was observed in either of the solvent media. In one experiment where *tert*-butanol was dissolved in water, a significant, dose-related increase in the number of revertants was produced, reaching almost two-fold the control value at a concentration of 2,250 µg/plate. It should be noted that DMSO is known to be a free radical scavenger, and its presence at high concentrations might mask a mutagenic response caused due to oxidative damage.

Mutagenicity of *tert*-butanol has been studied in other systems including *Neurospora crassa* and *Saccharomyces cerevisiae*. Yeast strain *Neurospora crassa* at the ad-3A locus (allele 38701) was used to test the mutagenic activity of *tert*-butanol at a concentration of 1.75 mol/L for 30 minutes. *tert*-Butanol did not induce reverse mutations in the tested strain at the exposed concentration ([Dickey et al., 1949](#)). On the other hand, *tert*-butanol, without exogenous metabolic activation, significantly increased the frequency of petite mutations (the mitochondrial deoxyribonucleic acid [DNA] deletion rho-) in *Saccharomyces cerevisiae* laboratory strains K5-A5, MMY1, D517-4B, and DS8 ([Jimenez et al., 1988](#)). This effect on mitochondrial DNA, also observed with ethanol and other solvents, was attributed by the study authors to the alteration in the lipid composition of mitochondrial membranes, and mitochondrial DNA's close association could be affected by membrane composition ([Jimenez et al., 1988](#)).

B.3.1.2. *In Vitro* Mammalian Studies

To understand the role of *tert*-butanol-induced genotoxicity in mammalian systems, in vitro studies have been conducted in different test systems and assays. *tert*-Butanol was tested to evaluate its ability to induce forward mutations at the thymidine kinase locus (tk) in the L5178Y tk+/- mouse lymphoma cells using forward mutation assay. Experiments were conducted both in the presence and absence of S9 metabolic activation. The mutant frequency was calculated using the ratio of mutant clones per plate/total clones per plate × 200. *tert*-Butanol did not reliably increase the frequency of forward mutations in L5178Y tk+/- mouse lymphoma cells with or without metabolic activation, although one experiment without addition of S9 yielded a small increase in mutant fraction at the highest tested concentration (5,000 µg/mL) ([McGregor et al., 1988](#)).

To further determine potential DNA and/or chromosomal damage induced by *tert*-butanol in in vitro systems, ([NTP, 1995](#)) studied sister chromatid exchanges (SCEs) and chromosomal aberrations (CAs). Chinese hamster ovary (CHO) cells were exposed to *tert*-butanol both in the

presence and absence of S9 activation at concentrations of 160–5,000 µg/mL for 26 hours. *tert*-Butanol did not induce SCEs in any of the concentrations tested, although in one experiment, there was a slight increase in percent relative change of SCEs per chromosome scored. The same authors also studied the effect of *tert*-butanol on CA formation. CHO cells were exposed to four concentrations (160, 500, 1,600, or 5,000 µg/mL) of *tert*-butanol both in the presence and absence of S9. No significant increase in CAs was observed in any of the concentrations tested. It should be noted that due to severe toxicity at the highest concentration (5,000 µg/mL), only 13 metaphase cells were scored instead of 100 in the chromosomal aberration assay.

[Sgambato et al. \(2009\)](#) examined the effects of *tert*-butanol on DNA damage using normal diploid rat fibroblast cell line. Cells were treated with 0- to 100-mM *tert*-butanol for 48 hours to determine the half maximal inhibitory concentration (IC₅₀; 0.44 ± 0.2 mM). The 48-hour IC₅₀ concentration was then used to determine DNA content, cell number, and phases of the cell cycle after 24 and 48 hours of exposure. Total protein and DNA oxidative damage were also measured. A comet assay was used to evaluate DNA fragmentation at time 0 and after 30 minutes, 4 hours, or 12 hours of exposure to the IC₅₀ concentration. *tert*-Butanol inhibited cell division in a dose-dependent manner as measured by the number of cells after 24 and 48 hours of exposure at IC₅₀ concentrations, as well as with concentrations at 1/10th the IC₅₀. There was no increase in cell death, suggesting a reduction in cell number due to reduced replication rather than cytotoxicity. *tert*-Butanol caused an accumulation in the G₀/G₁ phase of replication. These were related to different effects on the expression of *cyclin D1*, *p27Kip1*, and *p53* genes. An initial increase in DNA damage as measured by nuclear fragmentation was observed at the 30-minute timepoint. The DNA damage declined drastically after 4 hours and disappeared almost entirely after 12 hours of exposure to *tert*-butanol. This reduction in the extent of DNA fragmentation after the initial increase is likely the result of an efficient DNA repair mechanism activated by cells following DNA damage induced by *tert*-butanol.

DNA damage caused by *tert*-butanol was determined by single-cell gel electrophoresis (comet assay) in human promyelocytic leukemia (HL-60) cells. The cells were exposed to concentrations ranging from 1 to 30 mmol/L for 1 hour, and a total of 100 cells were evaluated for DNA fragmentation. A dose-dependent increase in DNA damage was observed between 1 and 30 mmol/L. No cytotoxicity was observed at the concentrations tested ([Tang et al. 1997](#)).

B.3.1.3. *In Vivo* Mammalian Studies

A limited number of *in vivo* studies are available to understand the role of *tert*-butanol on genotoxicity. The National Toxicology Program studied the effect of *tert*-butanol in a 13-week toxicity study ([NTP. 1995](#)). Peripheral blood samples were obtained from male and female B6CF1 mice that were exposed to *tert*-butanol in drinking water at doses of 3,000–40,000 ppm. Slides were prepared to determine the frequency of micronuclei in 10,000 normochromatic erythrocytes. In addition, the percentage of polychromatic erythrocytes among the total erythrocyte population was determined. No increase in micronucleus formation in peripheral blood lymphocytes was

1 observed either in male or female B6C3F₁ mice exposed for 13 weeks to *tert*-butanol in drinking
2 water at concentrations as high as 40,000 ppm (2,110 mg/kg-day) ([NTP, 1995](#)).

3 Male Kumming mice (8 per treatment) were administered 0, 0.099, 0.99, 10, 101, or
4 997 µg/kg bw ¹⁴C-*tert*-butanol in saline via gavage with specific activity ranging from 1.60 to
5 0.00978 mCi/mol ([Yuan et al., 2007](#)). Animals were sacrificed 6 hours after exposure, and liver,
6 kidney, and lung were collected. Tissues were prepared for DNA isolation with samples from the
7 same organs from every two mice combined. DNA adducts were measured using accelerated mass
8 spectrometry. The results of this study showed a dose-response increase in DNA adducts in all
9 three organs measured, although the methodology used to detect DNA adducts is considered
10 sensitive but may be nonspecific. The authors stated that *tert*-butanol was found, for the first time,
11 to form DNA adducts in mouse liver, lung, and kidney. Because this is a single and first-time study,
12 further validation of this study will provide certainty in understanding the mechanism of *tert*-
13 butanol-induced DNA adducts.
14

Table B-3. Summary of genotoxicity (both in vitro and in vivo) studies of tert-butanol.

Test system	Dose/Conc.	Results ^a		Comments	Reference
Bacterial Systems					
		-S9	+S9		
Reverse Mutation Assay <i>Salmonella typhimurium</i> (TA98, TA100, TA1535, TA1537, TA1538)	100, 333, 1000, 3333, 10,000 µg/plate	-	-	Preincubation procedure was followed. This study was part of the NTP 1995 testing results.	Zeiger et al. (1987);NTP (1995)
Reverse Mutation Assay <i>Salmonella typhimurium</i> (TA102)	1000–4000 µg/plate	ND	+	Only tested with S9 activation	Williams-Hill et al. (1999)
Reverse Mutation Assay <i>Salmonella typhimurium</i> (TA98, TA100, TA102, TA1535, TA1537)	5, 15, 50, 100, 150, 200, 500, 1000, 1500, 2500, 5000 µg/plate	-	-	Experiments conducted in two different laboratories, two vehicles – distilled water and DMSO were used, different concentrations were used in experiments from different laboratories	Mcgregor et al. (2005)
Reverse mutation <i>Neurospora crassa</i> , ad-3A locus (allele 38701)	1.75mol/L	-	-	Eighty four percent cell death was observed; note it is a 1949 study	Dickey et al. (1949)
Mitochondrial mutation <i>Saccharomyces cerevisiae</i> (K5-5A, MMY1, D517-4B, and DS8)	4.0% (vol/vol)	+ ^b	ND	Mitochondrial mutations, membrane solvent	Jimenez et al. (1988)
In vitro Systems					
Gene Mutation Assay, Mouse lymphoma cells L5178Y TK ^{+/-}	625, 1000, 1250, 2000, 3000, 4000, 5000 µg/mL	-	-	Cultures were exposed for 4 h, then cultured for 2 days before plating in soft agar with or without trifluorothymidine, 3 µg/mL; this study was part of the NTP 1995 testing results	McGregor et al. (1988);NTP (1995)
Sister-chromatid exchange, Chinese Hamster Ovary cells	160, 500, 1600, 2000, 3000, 4000, 5000 µg/mL	-	-	This study was part of the NTP 1995 testing results	Galloway, 1987; NTP (1995)
Chromosomal Aberrations, Chinese Hamster Ovary cells	160, 500, 1600, 2000, 3000, 4000, 5000 µg/mL	-	-	This study was part of the NTP 1995 testing results	Galloway, 1987 NTP (1995)
DNA damage (comet assay), Rat fibroblasts	0.44 mmol/L (IC ₅₀)	+ ^c	ND	Exposure duration – 30 min, 4 h, 12 h; this study provides other information on effect of cell cycle control genes and mechanism of action for TBA	Sgambato et al. (2009)

Test system	Dose/Conc.	Results ^a		Comments	Reference
DNA damage, (comet assay), human HL-60 leukemia cells	1, 5, 10, 30 mmol/L	+	ND	Exposure duration – 1h	Tang et al. (1997)
<i>In vivo Animal Studies</i>					
Micronucleus formation, B6C3F1 mouse peripheral blood cells	3000, 5000, 10,000, 20,000, 40,000 ppm	-		13-week, subchronic, drinking water study	NTP (1995)
DNA adducts, male Kunming mouse liver, kidney and lung cells	0.1–1000 µg/kg body weight	+		Gavage, 6-h exposure, DNA adduct determined by accelerator mass spectrometry	Yuan et al. (2007)

^a+ = positive; – = negative; ND = not determined.

^bEffect is predicted to be due to mitochondrial membrane composition.

^cDNA damage was completely reversed with increased exposure time.

B.3.2. Summary

tert-Butanol has been tested for its genotoxic potential using a variety of genotoxicity assays. Bacterial assays that detect reverse mutations have been thought to predict carcinogenicity with accuracy up to 80%. *tert*-Butanol did not induce mutations in most bacterial strains; however, when tested in TA102, a strain that is sensitive to damage at A-T sites inducible by oxidants, an increase in mutants was observed at low concentrations, although conflicting results were reported in another study. Furthermore, the solvent (e.g., distilled water or DMSO) used in the genotoxicity assay may impact results. In one experiment where *tert*-butanol was dissolved in distilled water, a significant, dose-related increase in the number of mutants was observed, with the maximum value reaching almost 2-fold the control value. DMSO is known to be a radical scavenger, and its presence in high concentrations might mask a mutagenic response modulated by oxidative damage. Other species such as *Neurospora crassa* did not produce reverse mutations as a result of exposure to *tert*-butanol.

tert-Butanol was tested in several human and animal in vitro mammalian systems for genotoxicity (gene mutation, sister chromatid exchanges, chromosomal aberrations, and DNA damage). No increase in gene mutations was observed in mouse lymphoma cells (L5178Y TK^{+/–}). These specific locus mutations in mammalian cells are used to demonstrate and quantify genetic damage, thereby confirming or extending the data obtained in the more widely used bacterial cell tests. Sister chromatid exchange or chromosomal aberrations were not observed in CHO cells in response to *tert*-butanol treatment. However, DNA damage was detected using comet assay in both rat fibroblasts and human HL-60 leukemia cells, with either an increase in DNA fragmentation at the beginning of the exposure or dose-dependent increase in DNA damage observed. An initial increase in DNA damage was observed at 30 minutes that declined drastically following 4 hours of exposure and disappeared almost entirely after 12 hours of exposure to *tert*-butanol. This reduction in the extent of DNA fragmentation after an initial increase is likely the result of an

1 efficient DNA repair mechanism activated by cells following DNA damage induced by *tert*-butanol. A
2 dose-dependent increase in DNA damage was observed in human cells tested; however, because
3 the exposure occurred for only 1 hour in this study, it is not possible to discern whether DNA-repair
4 mechanisms would occur after a longer period of observation.

5 Limited in vivo animal studies have been conducted on DNA adduct formation or
6 micronucleus formation. A dose-response increase in DNA adducts was observed in mouse liver,
7 kidney, and lung cells. The authors used accelerated mass spectrometry to detect DNA adducts, but
8 this method may be sensitive and not specific to the adducts in question. The method uses
9 ¹⁴C-labeled chemical for dosing, and the isolated DNA is oxidized to carbon dioxide and reduced to
10 filamentous graphite, and the ratios of ¹⁴C/¹²C are measured. The ratio is then converted to DNA
11 adducts based on nucleotide content of the DNA, hence the debate for the reliability of the data
12 obtained. Confirmation of this data will provide assurance in understanding the mechanism of
13 *tert*-butanol-induced DNA adducts. No increase in micronucleus formation was observed in mouse
14 peripheral blood cells in a 13-week drinking water study conducted by the National Toxicology
15 Program.

16 Overall, there is a limited database to understand the role of *tert*-butanol-induced
17 genotoxicity for mode of action and carcinogenicity. The database is limited either in terms of the
18 array of genotoxicity tests conducted or the number of studies within the same type of test. In
19 addition, the results are either conflicting or inconsistent. The test strains, solvents, or control for
20 volatility used in certain studies are variable and may impact results. Furthermore, in some studies,
21 the methodology used has been challenged for its specificity. Given the inconsistencies and
22 limitations of the database in terms of the methodology used, number of studies in the overall
23 database, coverage of studies across the genotoxicity battery, and the quality of the studies, the
24 weight of evidence analysis is inconclusive. The available data do not inform a definitive conclusion
25 on the genotoxicity of *tert*-butanol and thus the potential genotoxic effects of *tert*-butanol cannot be
26 discounted.

APPENDIX C. DOSE-RESPONSE MODELING FOR THE DERIVATION OF REFERENCE VALUES FOR EFFECTS OTHER THAN CANCER AND THE DERIVATION OF CANCER RISK ESTIMATES

C.1. BENCHMARK DOSE MODELING SUMMARY

This appendix provides technical detail on dose-response evaluation and determination of points of departure (PODs) for relevant endpoints. The endpoints were modeled using EPA's Benchmark Dose Software (BMDS), version 2.1.2. The preambles for the cancer and noncancer parts below describes the common practices used in evaluating the model fit and selecting the appropriate model for determining the POD as outlined in the *Benchmark Dose Technical Guidance Document* ([U.S. EPA, 2000](#)). In some cases, it may be appropriate to use alternative methods based on statistical judgment; exceptions are noted as necessary in the summary of the modeling results.

C.1.1. Noncancer Endpoints

C.1.1.1. Evaluation of Model Fit

For each dichotomous endpoint, BMDS dichotomous models were fitted to the data using the maximum likelihood method. Each model was tested for goodness-of-fit using a chi-square goodness-of-fit test (χ^2 p -value < 0.10 indicates lack of fit). Other factors were also used to assess model fit, such as scaled residuals, visual fit, and adequacy of fit in the low dose region and near the benchmark response (BMR).

For each continuous endpoint, BMDS continuous models were fitted to the data using the maximum likelihood method, and model fit was assessed by a series of tests. For each model, first the homogeneity of the variances was tested using a likelihood ratio test (BMDS Test 2). If Test 2 was not rejected (χ^2 p -value \geq 0.10), the model was fitted to the data assuming constant variance. If Test 2 was rejected (χ^2 p -value < 0.10), the variance was modeled as a power function of the mean, and the variance model was tested for adequacy of fit using a likelihood ratio test (BMDS Test 3). For fitting models using either constant variance or modeled variance, models for the mean response were tested for adequacy of fit using a likelihood ratio test (BMDS Test 4, with χ^2 p -value < 0.10 indicating inadequate fit). Other factors were also used to assess the model fit, such as scaled residuals, visual fit, and adequacy of fit in the low-dose region and near the BMR.

C.1.1.2. Model Selection

For each endpoint, the BMDL estimate (95% lower confidence limit on the BMD, as estimated by the profile likelihood method) and the Akaike's information criterion (AIC) value were

used to select a best-fit model from among the models exhibiting adequate fit. If the BMDL estimates were “sufficiently close,” that is, differed by at most 3-fold, the model selected was the one that yielded the lowest AIC value. If the BMDL estimates were not sufficiently close, the lowest BMDL was selected as the POD.

Table C-1. Non-cancer endpoints selected for dose-response modeling for tert-butanol

Endpoint/Study	Species / Sex	Doses and Effect Data						
		Dose (mg/kg-d)	0	90	200	420		
Kidney transitional epithelial hyperplasia NTP (1995)	Rat (F344) / Male	Dose (mg/kg-d)	0	90	200	420		
		Incidence / Total	25 / 50	32 / 50	36 / 50	40 / 50		
Kidney transitional epithelial hyperplasia NTP (1995)	Rat (F344) / Female	Dose (mg/kg-d)	0	180	330	650		
		Incidence / Total	0 / 50	0 / 50	3 / 50	17 / 50		
Mean relative kidney weight NTP (1995)	Rat (F344) / Male	Dose (mg/kg-d)	0	90	200	420		
		Mean ± SE (n)	3.68 ± 0.09 (10)	3.96 ± 0.13 (10)	4.22 ± 0.13 (10)	4.42 ± 0.15 (10)		
Mean relative kidney weight NTP (1995)	Rat (F344) / Female	Dose (mg/kg-d)	0	180	330	650		
		Mean ± SE (n)	3.49 ± 0.08 (10)	3.99 ± 0.07 (10)	4.21 ± 0.08 (10)	4.95 ± 0.17 (10)		
Kidney inflammation NTP (1995)	Rat (F344) / Female	Dose (mg/kg-d)	0	180	330	650		
		Incidence / Total	2 / 50	3 / 50	13 / 50	17 / 50		
Thyroid follicular cell hyperplasia NTP (1995)	Mouse (B6C3F ₁) / Male	Dose (mg/kg-d)	0	540	1,040	2,070		
		Incidence / Total	5 / 60	18 / 59	15 / 59	18 / 57		
Thyroid follicular cell hyperplasia NTP (1995)	Mouse (B6C3F ₁) / Female	Dose (mg/kg-d)	0	510	1,020	2,110		
		Incidence / Total	19 / 58	28 / 60	33 / 59	47 / 59		
Increased absolute kidney weight NTP (1997)	Rat (F344) / Male	Concentration (mg/m ³)	0	406	825	1643	3274	6369
		Mean ± SD (n)	1.21 ± 0.082 (10)	1.21 ± 0.096 (9)	1.18 ± 0.079 (10)	1.25 ± 0.111 (10)	1.34 ± 0.054 (10)	1.32 ± 0.089 (10)
Increased relative kidney weight NTP (1997)	Rat (F344) / Male	Concentration (mg/m ³)	0	406	825	1643	3274	6369
		Mean ± SD (n)	3.68 ± 0.253 (10)	3.71 ± 0.12 (9)	3.64 ± 0.126 (10)	3.76 ± 0.19 (10)	3.96 ± 0.158 (10)	4 ± 0.158 (10)

Endpoint/Study	Species / Sex	Doses and Effect Data						
		Concentration (mg/m ³)	0	406	825	1643	3274	6369
Increased absolute kidney weight NTP (1997)	Rat (F344) / Female	Mean ± SD (n)	0.817 ± 0.136 (10)	0.782 ± 0.063 (10)	0.821 ± 0.061 (10)	0.853 ± 0.045 (10)	0.831 ± 0.054 (10)	0.849 ± 0.038 (10)
		Concentration (mg/m ³)	0	406	825	1643	3274	6369
Increased relative kidney weight NTP (1997)	Rat (F344) / Female	Mean ± SD (n)	4.00 ± 0.474 (10)	3.98 ± 0.190 (10)	4.03 ± 0.158 (10)	4.14 ± 0.126 (10)	4.09 ± 0.190 (10)	4.35 ± 0.095 (10)
		Concentration (mg/m ³)	0	406	825	1643	3274	6369

C.1.1.3. Modeling Results

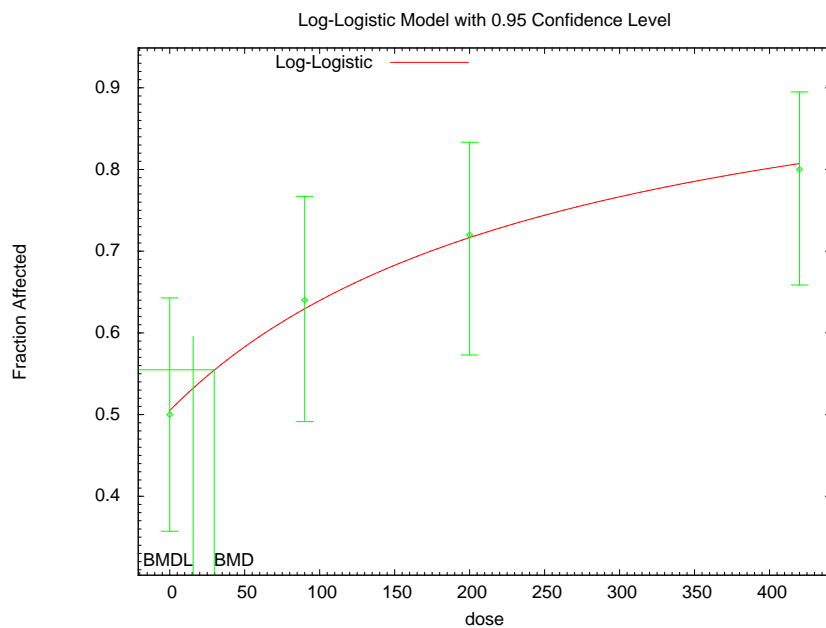
Below are tables summarizing the modeling results for the noncancer endpoints modeled. The following parameter restrictions were applied, unless otherwise noted.

- Dichotomous models: For the log-logistic and dichotomous Hill models, restrict slope ≥ 1; for the gamma and Weibull models, restrict power ≥ 1; for the multistage models, restrict beta values ≥ 0.
- Continuous models: For the polynomial models, restrict beta values ≥ 0; for the Hill, power, and exponential models, restrict power ≥ 1.

Table C-2. Summary of BMD modeling results for kidney transitional epithelial hyperplasia in male F344 rats exposed to *tert*-butanol in drinking water for 2 years ([NTP, 1995](#)); BMR = 10% extra risk.

Model ^a	Goodness of fit		BMD ₁₀ (mg/kg-d)	BMDL ₁₀ (mg/kg-d)	Basis for model selection
	p-value	AIC			
Log-logistic	0.976	248.0	30	16	Log-logistic model selected as best-fitting model based on lowest AIC with all BMDL values sufficiently close (BMDLs differed by slightly more than 3-fold).
Gamma	0.784	248.5	46	29	
Logistic	0.661	248.8	58	41	
Log-probit	0.539	249.2	84	53	
Multistage, 3°	0.784	248.5	46	29	
Probit	0.633	248.9	60	43	
Weibull	0.784	248.5	46	29	
Dichotomous-Hill	0.968	250.0	25	15	

^aScaled residuals for selected model for doses 0, 90, 200, and 420 mg/kg-d were -0.076, 0.147, 0.046, and -0.137, respectively.



17:16 05/13 2011

Figure C-1. Plot of mean response by dose, with fitted curve for selected model.

```

=====
Logistic Model. (Version: 2.13; Date: 10/28/2009)
Input Data File: M:\NCEA t-Butanol\BMD modeling\BMDS Output\17 NTP 1995b_Kidney
transitional epithelial hyperplasia, male rats_LogLogistic_10.(d)
Gnuplot Plotting File: M:\NCEA t-Butanol\BMD modeling\BMDS Output\17 NTP
1995b_Kidney transitional epithelial hyperplasia, male rats_LogLogistic_10.plt
Fri May 13 17:16:25 2011
=====

```

[notes]

The form of the probability function is:

$$P[\text{response}] = \text{background} + (1 - \text{background}) / [1 + \text{EXP}(-\text{intercept} - \text{slope} * \text{Log}(\text{dose}))]$$

Dependent variable = Incidence

Independent variable = Dose

Slope parameter is restricted as slope >= 1

Total number of observations = 4

Total number of records with missing values = 0

Maximum number of iterations = 250

Relative Function Convergence has been set to: 1e-008

Parameter Convergence has been set to: 1e-008

User has chosen the log transformed model

Default Initial Parameter Values

```

background = 0.5
intercept = -5.54788
slope = 1

```

Asymptotic Correlation Matrix of Parameter Estimates

(*** The model parameter(s) -slope
have been estimated at a boundary point, or have been specified by the user,
and do not appear in the correlation matrix)

```

background  intercept
background  1      -0.71
intercept  -0.71    1

```

Parameter Estimates

Variable	Estimate	Std. Err.	95.0% Wald Confidence Interval	
			Lower Conf. Limit	Upper Conf. Limit
background	0.505366	*	*	*
intercept	-5.58826	*	*	*
slope	1	*	*	*

* - Indicates that this value is not calculated.

Analysis of Deviance Table

Model	Log(likelihood)	# Param's	Deviance Test	d.f.	P-value
Full model	-121.996	4			
Fitted model	-122.02	2	0.048148	2	0.9762
Reduced model	-127.533	1	11.0732	3	0.01134

This document is a draft for review purposes only and does not constitute Agency policy.

AIC: 248.04

Goodness of Fit

Dose	Est._Prob.	Expected	Scaled Observed	Size	Residual
0.0000	0.5054	25.268	25.000	50	-0.076
90.0000	0.6300	31.498	32.000	50	0.147
200.0000	0.7171	35.854	36.000	50	0.046
420.0000	0.8076	40.382	40.000	50	-0.137

Chi^2 = 0.05 d.f. = 2 P-value = 0.9762

Benchmark Dose Computation

Specified effect = 0.1

Risk Type = Extra risk

Confidence level = 0.95

BMD = 29.6967

BMDL = 15.6252

Table C-3. Summary of BMD modeling results for kidney transitional epithelial hyperplasia in female F344 rats exposed to *tert*-butanol in drinking water for 2 years ([NTP, 1995](#)); BMR = 10% extra risk.

Model ^a	Goodness of fit		BMD ₁₀ (mg/kg-d)	BMDL ₁₀ (mg/kg-d)	Basis for model selection
	p-value	AIC			
Gamma	0.83	91.41	409	334	Multistage 3 rd order model selected as best-fitting model based on lowest AIC with all BMDL values sufficiently close (BMDLs differed by less than 3-fold).
Logistic	0.50	92.81	461	393	
LogLogistic	0.79	91.57	414	333	
LogProbit	0.89	91.19	400	327	
Multistage 3^o	0.92	89.73	412	339	
Probit	0.62	92.20	439	372	
Weibull	0.76	91.67	421	337	
Dichotomous-Hill	N/A ^b	117.89	Error ^c	Error ^c	

^aScaled residuals for selected model for doses 0, 180, 330, and 650 mg/m³ were 0.0, -0.664, 0.230, and 0.016, respectively.

^bNo available degrees of freedom to estimate a p-value.

^cBMD and BMDL computation failed for the Dichotomous-Hill model.

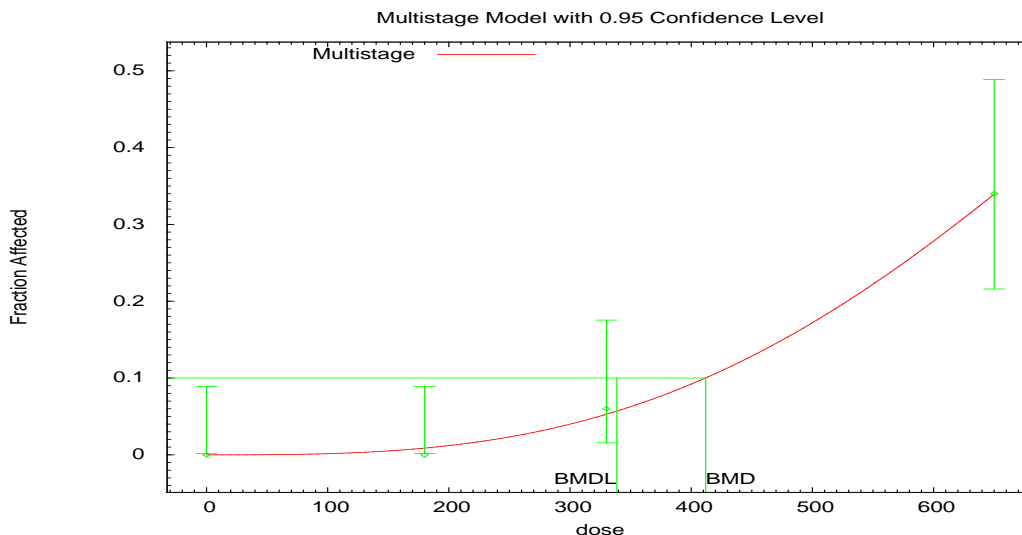


Figure C-2. Plot of mean response by dose, with fitted curve for selected model.

```
=====
Multistage Model. (Version: 3.2; Date: 05/26/2010)
Input Data File: M:\NCEA tert-butanol\BMD modeling\BMDS Output\20 NTP
1995b_Kidney transitional epithelial hyperplasia, female rats_Multi3_10.(d)
Gnuplot Plotting File: M:\NCEA tert-butanol\BMD modeling\BMDS Output\20 NTP
1995b_Kidney transitional epithelial hyperplasia, female rats_Multi3_10.plt
Mon May 09 18:31:33 2011
=====
```

[notes]

The form of the probability function is:

$$P[\text{response}] = \text{background} + (1 - \text{background}) * [1 - \exp(-\beta_1 \text{dose} - \beta_2 \text{dose}^2 - \beta_3 \text{dose}^3)]$$

The parameter betas are restricted to be positive

Dependent variable = Incidence
Independent variable = Dose

Total number of observations = 4
Total number of records with missing values = 0
Total number of parameters in model = 4
Total number of specified parameters = 0
Degree of polynomial = 3

Maximum number of iterations = 250
Relative Function Convergence has been set to: 1e-008
Parameter Convergence has been set to: 1e-008

Default Initial Parameter Values

Background = 0
Beta(1) = 0
Beta(2) = 1.51408e-007
Beta(3) = 1.29813e-009

Asymptotic Correlation Matrix of Parameter Estimates

This document is a draft for review purposes only and does not constitute Agency policy.

```

( *** The model parameter(s) -Background -Beta(1) -Beta(2)
      have been estimated at a boundary point, or have been specified by the user,
      and do not appear in the correlation matrix )

Beta(3)

Beta(3)      1

Parameter Estimates

Variable      Estimate      95.0% Wald Confidence Interval
Background      0      *      *      *
Beta(1)          0      *      *      *
Beta(2)          0      *      *      *
Beta(3)  1.50711e-009      *      *      *

* - Indicates that this value is not calculated.

Analysis of Deviance Table

Model  Log(likelihood)  # Param's  Deviance Test  d.f.  P-value
Full model      -43.4002      4
Fitted model    -43.8652      1      0.9301      3      0.8182
Reduced model    -65.0166      1      43.2329      3      <.0001

AIC:      89.7304

Goodness of Fit

Dose  Est._Prob.  Expected  Scaled Observed  Size  Residual
-----
0.0000  0.0000      0.000      0.000      50      0.000
180.0000  0.0088      0.438      0.000      50      -0.664
330.0000  0.0527      2.636      3.000      50      0.230
650.0000  0.3389     16.946     17.000      50      0.016

Chi^2 = 0.49   d.f. = 3   P-value = 0.9200

Benchmark Dose Computation

Specified effect =      0.1

Risk Type      =      Extra risk

Confidence level =      0.95

BMD =      411.95

BMDL =      338.618

BMDU =      469.73

Taken together, (338.618, 469.73 ) is a 90 % two-sided confidence
interval for the BMD

```

Table C-4. Summary of BMD modeling results for relative kidney weights in male F344 rats exposed to *tert*-butanol in drinking water for 15 months ([NTP, 1995](#)); BMR = 10% relative deviation and 1 standard deviation.

Model ^a	Goodness of fit		BMD _{10%} (mg/kg-d)	BMDL _{10%} (mg/kg-d)	BMD _{1SD} (mg/kg-d)	BMDL _{1SD} (mg/kg-d)	Basis for model selection
	<i>p</i> -value	AIC					
Hill	NA	-27.27	120	39	124	45	Exponential (M4) is selected as the best-fitting model based on visual fit at the low-dose region.
Exponential (M4)	0.854	-29.23	117	48	123	53	
Exponential (M5)	N/A	-27.27	121	48	126	54	
Linear	0.421	-29.54	222	155	229	161	
Polynomial	0.421	-29.54	222	155	229	161	
Power	0.421	-29.54	222	155	229	161	
Exponential (M2)	0.365	-29.25	236	170	243	176	
Exponential (M3)	0.365	-29.25	236	170	243	176	

^aConstant variance case presented (BMD Test 2 *p*-value = 0.466), selected model in bold; scaled residuals for selected model for doses 0, 90, 200, 420 mg/kg-d were 0.04009, -0.1264, 0.122, and -0.03578, respectively.

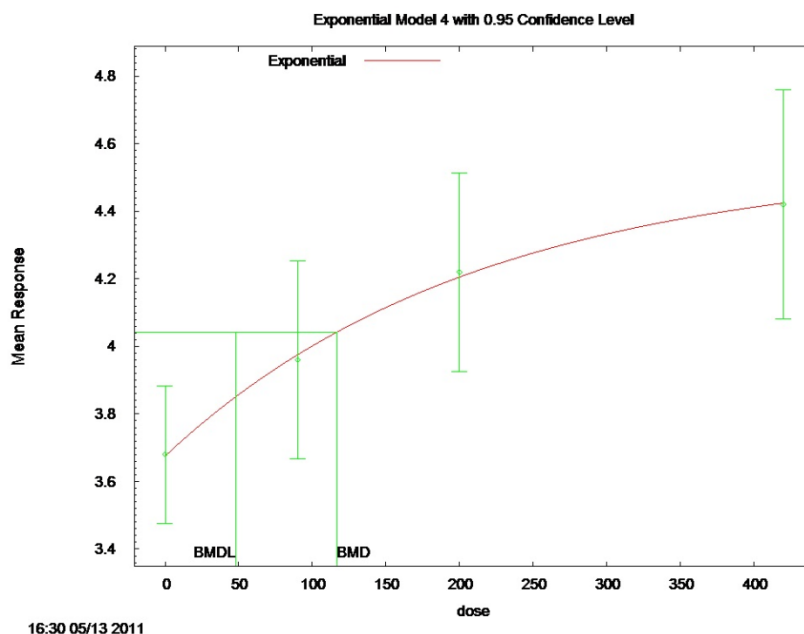


Figure C-3. Plot of mean response by dose, with fitted curve for selected model (10% relative deviation).

```
=====
Exponential Model. (Version: 1.7; Date: 12/10/2009)
Input Data File: M:\NCEA t-Butanol\BMD modeling\BMDs Output\21 NTP
1995b_Mean relative kidney weight, male rats_ExpCV_10RD.(d)
Gnuplot Plotting File: M:\NCEA t-Butanol\BMD modeling\BMDs Output\21 NTP
1995b_Mean relative kidney weight, male rats_ExpCV_10RD.plt
Fri May 13 16:30:21 2011
=====
```

[notes]

The form of the response function by Model:

```
Model 2: Y[dose] = a * exp{sign * b * dose}
Model 3: Y[dose] = a * exp{sign * (b * dose)^d}
Model 4: Y[dose] = a * [c-(c-1) * exp{-b * dose}]
Model 5: Y[dose] = a * [c-(c-1) * exp{-(b * dose)^d}]
```

Note: Y[dose] is the median response for exposure = dose;
 sign = +1 for increasing trend in data;
 sign = -1 for decreasing trend.

Model 2 is nested within Models 3 and 4.
 Model 3 is nested within Model 5.
 Model 4 is nested within Model 5.

Dependent variable = Response
 Independent variable = Dose
 Data are assumed to be distributed: normally
 Variance Model: $\exp(\ln\alpha + \rho * \ln(Y[dose]))$
 rho is set to 0.
 A constant variance model is fit.

Total number of dose groups = 4
 Total number of records with missing values = 0
 Maximum number of iterations = 250
 Relative Function Convergence has been set to: 1e-008
 Parameter Convergence has been set to: 1e-008

This document is a draft for review purposes only and does not constitute Agency policy.

MLE solution provided: Exact

Initial Parameter Values

Variable	Model 4
-----	-----
lnalpha	-1.93171
rho(S)	0
a	3.496
b	0.00417714
c	1.32752
d	1

(S) = Specified

Parameter Estimates

Variable	Model 4
-----	-----
lnalpha	-1.93087
rho	0
a	3.67517
b	0.00469937
c	1.23673
d	1

Table of Stats From Input Data

Dose	N	Obs Mean	Obs Std Dev
-----	---	-----	-----
0	10	3.68	0.2846
90	10	3.96	0.4111
200	10	4.22	0.4111
420	10	4.42	0.4743

Estimated Values of Interest

Dose	Est Mean	Est Std	Scaled Residual
-----	-----	-----	-----
0	3.675	0.3808	0.04009
90	3.975	0.3808	-0.1264
200	4.205	0.3808	0.1221
420	4.424	0.3808	-0.03578

Other models for which likelihoods are calculated:

Model A1: $Y_{ij} = \mu(i) + e(ij)$
 $\text{Var}\{e(ij)\} = \sigma^2$

Model A2: $Y_{ij} = \mu(i) + e(ij)$
 $\text{Var}\{e(ij)\} = \sigma(i)^2$

Model A3: $Y_{ij} = \mu(i) + e(ij)$
 $\text{Var}\{e(ij)\} = \exp(\ln\alpha + \log(\text{mean}(i)) * \rho)$

Model R: $Y_{ij} = \mu + e(i)$
 $\text{Var}\{e(ij)\} = \sigma^2$

Likelihoods of Interest

Model	Log(likelihood)	DF	AIC
-----	-----	----	-----

This document is a draft for review purposes only and does not constitute Agency policy.

A1	18.63423	5	-27.26846
A2	19.91058	8	-23.82116
A3	18.63423	5	-27.26846
R	10.08355	2	-16.1671
4	18.61733	4	-29.23465

Additive constant for all log-likelihoods = -36.76. This constant added to the above values gives the log-likelihood including the term that does not depend on the model parameters.

Explanation of Tests

Test 1: Does response and/or variances differ among Dose levels? (A2 vs. R)

Test 2: Are Variances Homogeneous? (A2 vs. A1)

Test 3: Are variances adequately modeled? (A2 vs. A3)

Test 6a: Does Model 4 fit the data? (A3 vs 4)

Tests of Interest

Test	-2*log(Likelihood Ratio)	D. F.	p-value
Test 1	19.65	6	0.00319
Test 2	2.553	3	0.4658
Test 3	2.553	3	0.4658
Test 6a	0.03381	1	0.8541

The p-value for Test 1 is less than .05. There appears to be a difference between response and/or variances among the dose levels, it seems appropriate to model the data.

The p-value for Test 2 is greater than .1. A homogeneous variance model appears to be appropriate here.

The p-value for Test 3 is greater than .1. The modeled variance appears to be appropriate here.

The p-value for Test 6a is greater than .1. Model 4 seems to adequately describe the data.

Benchmark Dose Computations:

Specified Effect = 0.100000

Risk Type = Relative deviation

Confidence Level = 0.950000

BMD = 116.807

BMDL = 48.0466

Table C-5. Summary of BMD modeling results for relative kidney weights in female F344 rats exposed to *tert*-butanol in drinking water for 15 months (NTP, 1995); BMR = 10% relative deviation and 1 standard deviation.

Model ^a	Goodness of fit		BMD _{10%} (mg/kg-d)	BMDL _{10%} (mg/kg-d)	BMD _{1SD} (mg/kg-d)	BMDL _{1SD} (mg/kg-d)	Basis for model selection
	<i>p</i> -value	AIC					
Exponential (M2) Exponential (M3)	0.48	-49.14	178	154	108	80	The linear model was selected on the basis of the lowest AIC with all BMDL values for fitting models being sufficiently close (BMDLs differed by less than 3-fold).
Exponential (M4) Exponential (M5)	0.33	-47.64	154	107	90	56	
Hill	0.33	-47.64	154	105	90	Error ^b	
Linear Power	0.62	-49.63	158	133	92	68	
Polynomial 3°	0.33	-47.63	158	133	98	68	

^aModeled variance case presented (BMD Test 2 *p*-value = 0.0091), selected model in bold; scaled residuals for selected model for doses 0, 180, 330, and 650 mg/kg-d were -0.383, 0.887, -0.411, and -0.105, respectively.

^bThe BMDL_{1SD} computation failed for the Hill model.

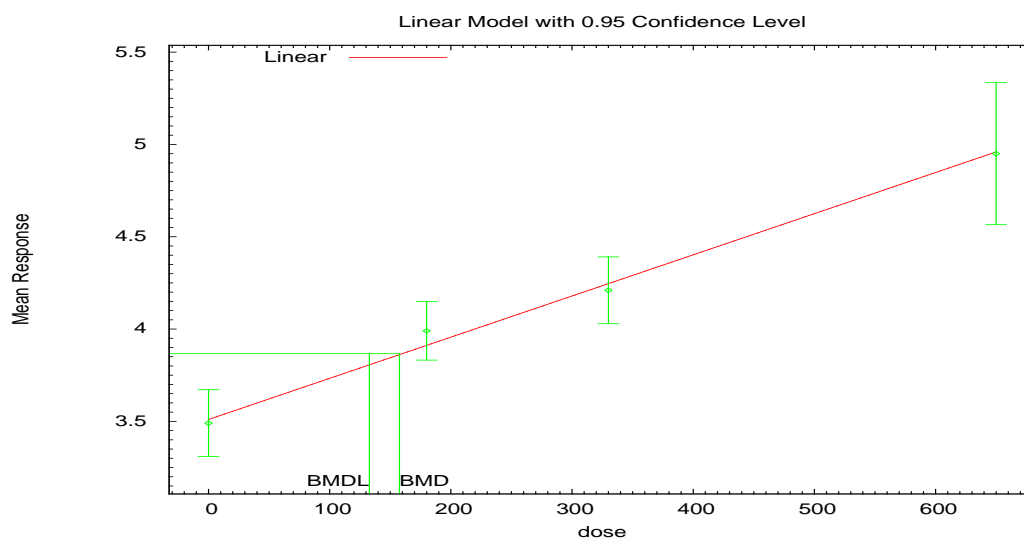


Figure C-4. Plot of mean response by dose, with fitted curve for selected model (10% relative deviation).

```

=====
Polynomial Model. (Version: 2.16; Date: 05/26/2010)
Input Data File: M:\NCEA tert-butanol\BMD modeling\BMDs Output\23 NTP 1995b_Mean
relative kidney weight, female rats_Linear_10RD.(d)

```

Supplemental Information—tert Butanol

Gnuplot Plotting File: M:\NCEA *tert-butanol*\BMD modeling\BMDs Output\23 NTP
1995b_Mean relative kidney weight, female rats_Linear_10RD.plt
Mon May 09 18:34:15 2011

[notes]

The form of the response function is:

$Y[\text{dose}] = \text{beta}_0 + \text{beta}_1 \cdot \text{dose} + \text{beta}_2 \cdot \text{dose}^2 + \dots$

Dependent variable = Response

Independent variable = Dose

Signs of the polynomial coefficients are not restricted

The variance is to be modeled as $\text{Var}(i) = \exp(\text{lalpha} + \log(\text{mean}(i)) \cdot \text{rho})$

Total number of dose groups = 4

Total number of records with missing values = 0

Maximum number of iterations = 250

Relative Function Convergence has been set to: 1e-008

Parameter Convergence has been set to: 1e-008

Default Initial Parameter Values

lalpha = -2.14986

rho = 0

beta_0 = 3.52312

beta_1 = 0.00219613

Asymptotic Correlation Matrix of Parameter Estimates

	lalpha	rho	beta_0	beta_1
lalpha	1	-1	0.1	-0.14
rho	-1	1	-0.1	0.14
beta_0	0.1	-0.1	1	-0.66
beta_1	-0.14	0.14	-0.66	1

Parameter Estimates

Variable	Estimate	Std. Err.	95.0% Wald Confidence Interval	
			Lower Conf. Limit	Upper Conf. Limit
lalpha	-8.78559	2.23999	-13.1759	-4.39529
rho	4.47471	1.57167	1.39429	7.55513
beta_0	3.51492	0.0580177	3.40121	3.62864
beta_1	0.00223049	0.00022176	0.00179585	0.00266513

Table of Data and Estimated Values of Interest

Dose	N	Obs Mean	Est Mean	Obs Std Dev	Est Std Dev	Scaled Res.
0	10	3.49	3.51	0.253	0.206	-0.383
180	10	3.99	3.92	0.221	0.262	0.887
330	10	4.21	4.25	0.253	0.315	-0.411
650	10	4.95	4.96	0.538	0.446	-0.105

This document is a draft for review purposes only and does not constitute Agency policy.

Model Descriptions for likelihoods calculated

Model A1: $Y_{ij} = \mu(i) + e(ij)$
 $\text{Var}\{e(ij)\} = \sigma^2$

Model A2: $Y_{ij} = \mu(i) + e(ij)$
 $\text{Var}\{e(ij)\} = \sigma(i)^2$

Model A3: $Y_{ij} = \mu(i) + e(ij)$
 $\text{Var}\{e(ij)\} = \exp(\alpha + \rho \ln(\mu(i)))$
 Model A3 uses any fixed variance parameters that were specified by the user

Model R: $Y_i = \mu + e(i)$
 $\text{Var}\{e(i)\} = \sigma^2$

Likelihoods of Interest

Model	Log(likelihood)	# Param's	AIC
A1	25.104490	5	-40.208981
A2	30.882250	8	-45.764500
A3	29.295765	6	-46.591531
fitted	28.815603	4	-49.631206
R	-0.698257	2	5.396514

Explanation of Tests

Test 1: Do responses and/or variances differ among Dose levels?
 (A2 vs. R)

Test 2: Are Variances Homogeneous? (A1 vs A2)

Test 3: Are variances adequately modeled? (A2 vs. A3)

Test 4: Does the Model for the Mean Fit? (A3 vs. fitted)

(Note: When $\rho=0$ the results of Test 3 and Test 2 will be the same.)

Tests of Interest

Test	$-2 \times \log(\text{Likelihood Ratio})$	Test df	p-value
Test 1	63.161	6	<.0001
Test 2	11.5555	3	0.009072
Test 3	3.17297	2	0.2046
Test 4	0.960325	2	0.6187

The p-value for Test 1 is less than .05. There appears to be a difference between response and/or variances among the dose levels. It seems appropriate to model the data.

The p-value for Test 2 is less than .1. A non-homogeneous variance model appears to be appropriate.

The p-value for Test 3 is greater than .1. The modeled variance appears to be appropriate here.

The p-value for Test 4 is greater than .1. The model chosen seems to adequately describe the data.

Benchmark Dose Computation

Specified effect = 0.1

Risk Type = Relative risk

Confidence level = 0.95

BMD = 157.585

BMDL = 132.699

Table C-6. Summary of BMD modeling results for kidney inflammation in female rats exposed to *tert*-butanol in drinking water for 2 years (NTP, 1995); BMR = 10% extra risk.

Model ^a	Goodness of fit		BMD _{10%} (mg/kg-d)	BMDL _{10%} (mg/kg-d)	Basis for model selection
	p-value	AIC			
Gamma	0.084	169.9	231	135	LogProbit was selected on the basis of the lowest AIC with all BMDL values for fitting models being sufficiently close (BMDLs differed by less than 3-fold).
Logistic	0.082	169.7	305	252	
LogLogistic	0.092	169.8	228	124	
LogProbit	0.243	167.6	254	200	
Multistage 3°	0.072	170.3	216	132	
Probit	0.108	169.2	285	235	
Weibull	0.081	170.0	226	134	
Dichotomous-Hill	N/A ^b	169.5	229	186	

^aSelected model in bold; scaled residuals for selected model for doses 0, 180, 330, and 650 mg/kg-d were -0.067, -0.700, 1.347, and -0.724, respectively.

^bNo available degrees of freedom to estimate a *p*-value.

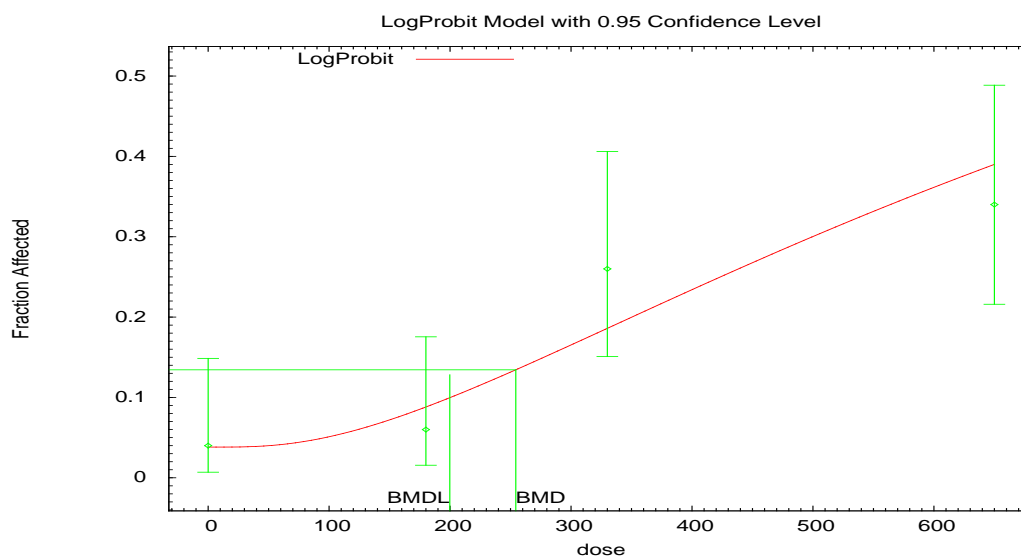


Figure C-5. Plot of mean response by dose, with fitted curve for selected model.

```
=====
Probit Model. (Version: 3.2; Date: 10/28/2009)
Input Data File: M:/NCEA tert-butanol/BMD modeling/BMDS Output/19 NTP
1995b_Kidney inflammation, female rats_LogProbit_10.(d)
Gnuplot Plotting File: M:/NCEA tert-butanol/BMD modeling/BMDS Output/19 NTP
1995b_Kidney inflammation, female rats_LogProbit_10.plt
Fri May 13 17:17:59 2011
=====
```

[notes]

The form of the probability function is:

$$P[\text{response}] = \text{Background} + (1 - \text{Background}) * \text{CumNorm}(\text{Intercept} + \text{Slope} * \text{Log}(\text{Dose})),$$

where CumNorm(.) is the cumulative normal distribution function

Dependent variable = Incidence

Independent variable = Dose

Slope parameter is restricted as slope >= 1

Total number of observations = 4

Total number of records with missing values = 0

Maximum number of iterations = 250

Relative Function Convergence has been set to: 1e-008

Parameter Convergence has been set to: 1e-008

User has chosen the log transformed model

Default Initial (and Specified) Parameter Values

background = 0.04

intercept = -8.01425

slope = 1.18928

Asymptotic Correlation Matrix of Parameter Estimates

(*** The model parameter(s) -slope
have been estimated at a boundary point, or have been specified by the user,
and do not appear in the correlation matrix)

	background	intercept
background	1	-0.51
intercept	-0.51	1

Parameter Estimates

Variable	Estimate	Std. Err.	95.0% Wald Confidence Interval	
			Lower Conf. Limit	Upper Conf. Limit
background	0.0381743	0.0246892	-0.0102155	0.0865642
intercept	-6.82025	0.161407	-7.1366	-6.5039
slope	1	NA		

NA - Indicates that this parameter has hit a bound
implied by some inequality constraint and thus
has no standard error.

Analysis of Deviance Table

Model	Log(likelihood)	# Param's	Deviance Test	d.f.	P-value
Full model	-80.4502	4			
Fitted model	-81.8218	2	2.7432	2	0.2537
Reduced model	-92.7453	1	24.5902	3	<.0001

AIC: 167.644

Supplemental Information—tert Butanol

Goodness of Fit					
Dose	Est._Prob.	Expected	Scaled	Size	Residual
			Observed		
0.0000	0.0382	1.909	2.000	50	0.067
180.0000	0.0880	4.402	3.000	50	-0.700
330.0000	0.1859	9.295	13.000	50	1.347
650.0000	0.3899	19.495	17.000	50	-0.724
Chi^2 = 2.83 d.f. = 2 P-value = 0.2427					
Benchmark Dose Computation					
Specified effect = 0.1					
Risk Type = Extra risk					
Confidence level = 0.95					
BMD = 254.347					
BMDL = 199.789					

Table C-7. Summary of BMD modeling results for thyroid follicular cell hyperplasia in male B6C3F1 mice exposed to *tert*-butanol in drinking water for 2 years ([NTP, 1995](#)); BMR = 10% extra risk.

Model ^a	Goodness of fit		BMD _{10%} (mg/kg-d)	BMDL _{10%} (mg/kg-d)	Basis for model selection
	p-value	AIC			
Gamma	0.052	254.7	702	430	No model was selected as a best-fitting model as models did not fit the overall goodness-of-fit criterion.
Logistic	0.031	256.1	1,064	751	
LogLogistic	0.069	254.1	586	340	
LogProbit	0.012	258.2	1,320	810	
Multistage 3° Weibull	0.052	254.7	702	430	
Probit	0.032	255.9	1,020	713	
Dichotomous-Hill	N/A ^b	253.6	0.19	Error ^c	

^aNo model was selected as a best-fitting model.

^bNo available degrees of freedom to estimate a *p*-value.

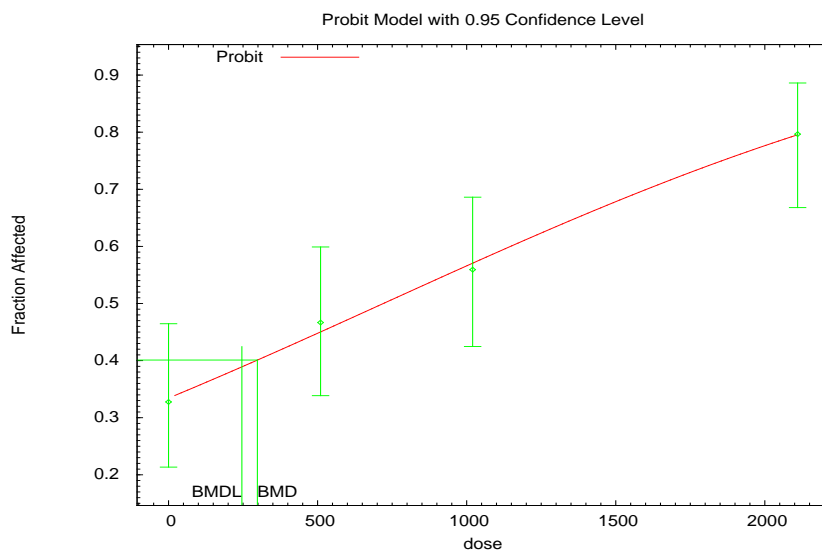
^cBMDL computation failed for the Dichotomous-Hill model.

Table C-8. Summary of BMD modeling results for thyroid follicular cell hyperplasia in female B6C3F1 mice exposed to *tert*-butanol in drinking water for 2 years ([NTP, 1995](#)); BMR = 10% extra risk.

Model ^a	Goodness of fit		BMD ₁₀ (mg/kg-d)	BMDL ₁₀ (mg/kg-d)	Basis for model selection
	p-value	AIC			
Gamma	0.63	303.1	327	154	The probit model was selected on the basis of the lowest AIC with all BMDL values for fitting models being sufficiently close (BMDLs differed by less than 3-fold).
Logistic	0.94	301.0	297	243	
LogLogistic	0.52	303.2	375	115	
LogProbit	0.48	303.3	388	277	
Multistage 3°	0.81	302.9	269	155	
Probit	0.95	300.9	298	246	
Weibull	0.66	303.0	321	154	
Dichotomous-Hill	0.66	27,226	Error ^b	Error ^b	

^aSelected model in bold; scaled residuals for selected model for doses 0, 510, 1,020, and 2,110 mg/kg-d were -0.110, 0.255, -0.174, and 0.025, respectively.

^bThe BMD and BMDL computations failed for the Dichotomous-Hill model.



18:36 05/09 2011

Figure C-6. Plot of mean response by dose, with fitted curve for selected model.

```

=====
Probit Model. (Version: 3.2; Date: 10/28/2009)
Input Data File: M:\NCEA tert-butanol\BMD modeling\BMDS Output\27 NTP
1995b_Thyroid follicular cell hyperplasia, female mice_Probit_10.(d)
Gnuplot Plotting File: M:\NCEA tert-butanol\BMD modeling\BMDS Output\27 NTP
1995b_Thyroid follicular cell hyperplasia, female mice_Probit_10.plt
Mon May 09 18:36:50 2011

```

This document is a draft for review purposes only and does not constitute Agency policy.

[notes]

The form of the probability function is:

$P[\text{response}] = \text{CumNorm}(\text{Intercept} + \text{Slope} * \text{Dose}),$

where $\text{CumNorm}(\cdot)$ is the cumulative normal distribution function

Dependent variable = Incidence

Independent variable = Dose

Slope parameter is not restricted

Total number of observations = 4

Total number of records with missing values = 0

Maximum number of iterations = 250

Relative Function Convergence has been set to: 1e-008

Parameter Convergence has been set to: 1e-008

Default Initial (and Specified) Parameter Values

background = 0 Specified

intercept = -0.425261

slope = 0.000589168

Asymptotic Correlation Matrix of Parameter Estimates

(*** The model parameter(s) -background
have been estimated at a boundary point, or have been specified by the user,
and do not appear in the correlation matrix)

	intercept	slope
intercept	1	-0.76
slope	-0.76	1

Parameter Estimates

Variable	Estimate	Std. Err.	95.0% Wald Confidence Interval	Lower Conf. Limit	Upper Conf. Limit
intercept	-0.427828	0.129459	-0.681563	-0.174092	
slope	0.000593756	0.00011419	0.000369947	0.000817564	

Analysis of Deviance Table

Model	Log(likelihood)	# Param's	Deviance Test	d.f.	P-value
Full model	-148.416	4			
Fitted model	-148.47	2	0.108205	2	0.9473
Reduced model	-162.896	1	28.9589	3	<.0001

AIC: 300.941

Goodness of Fit

Dose	Est._Prob.	Expected	Scaled Observed	Size	Residual
0.0000	0.3344	19.395	19.000	58	-0.110
510.0000	0.4503	27.015	28.000	60	0.255
1020.0000	0.5706	33.663	33.000	59	-0.174
2110.0000	0.7953	46.923	47.000	59	0.025

This document is a draft for review purposes only and does not constitute Agency policy.

Supplemental Information—tert Butanol

Chi² = 0.11 d.f. = 2 P-value = 0.9473

Benchmark Dose Computation

Specified effect = 0.1

Risk Type = Extra risk

Confidence level = 0.95

BMD = 297.997

BMDL = 246.075

Table C-9. Summary of BMD modeling results for absolute kidney weight in male F344 rats exposed to *tert*-butanol via inhalation for 6 hr/d, 5d/wk for 13 weeks (NTP, 1997); BMR = 10% relative deviation from the mean.

Model ^a	Goodness of fit		BMC _{10RD} (mg/m ³)	BMCL _{10RD} (mg/m ³)	Basis for model selection
	<i>p</i> -value	AIC			
Exponential (M2)	<0.0001	-205.06	error ^b	error ^b	The Hill model was selected as the only adequately-fitting model.
Exponential (M3)	<0.0001	-203.06	9.2E+07	7094	
Exponential (M4)	<0.0001	-203.06	error ^b	0	
Exponential (M5)	<0.0001	-201.06	error ^b	0	
Hill	0.763	-226.82	1931	1705	
Power ^c	0.0607	-220.97	5364	3800	
Linear					
Polynomial 5 ^d Polynomial 4 ^e Polynomial 3 ^o	1.44E-04	-207.06	-9999	error ^f	
Polynomial 2 ^o	1.44E-04	-207.06	-9999	18436	

^a Constant variance case presented (BMD Test 2 *p*-value = 0.390), selected model in bold; scaled residuals for selected model for doses 0, 406, 825, 1643, 3274, and 6369 mg/m³ were 0.395, 0.374, -0.75, -1.96e-006, 0.381, and -0.381, respectively.

^b BMC or BMCL computation failed for this model.

^c For the Power model, the power parameter estimate was 1. The models in this row reduced to the Linear model.

^d For the Polynomial 5^o model, the b5 and b4 coefficient estimates were 0 (boundary of parameters space). The models in this row reduced to the Polynomial 3^o model.

^e For the Polynomial 4^o model, the b4 coefficient estimate was 0 (boundary of parameters space). The models in this row reduced to the Polynomial 3^o model.

^f BMC or BMCL computation failed for this model

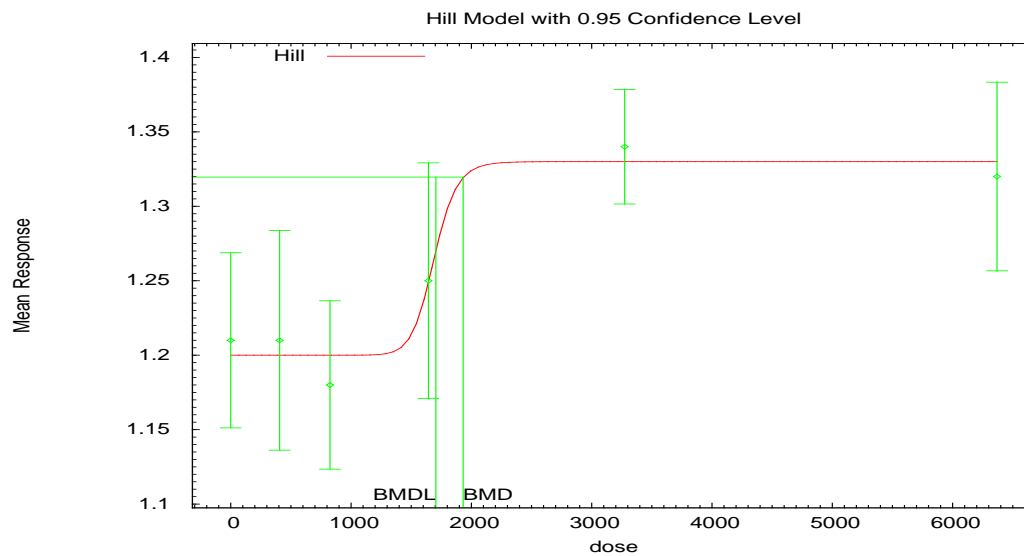


Figure C-7. Plot of mean response by dose, with fitted curve for selected model; dose shown in mg/m³.

Hill Model. (Version: 2.15; Date: 10/28/2009)

The form of the response function is: $Y[\text{dose}] = \text{intercept} + v \cdot \text{dose}^n / (k^n + \text{dose}^n)$

A constant variance model is fit

Benchmark Dose Computation.

BMR = 10% Relative risk

BMD = 1931.35

BMDL at the 95% confidence level = 1704.82

Parameter Estimates

Variable	Estimate	Default Initial Parameter Values
alpha	0.00687349	0.00750263
rho	n/a	0
intercept	1.19966	1.21
v	0.130345	0.13
n	18	18
k	1685.82	4451.94

Table of Data and Estimated Values of Interest

Dose	N	Obs Mean	Est Mean	Obs Std Dev	Est Std Dev	Scaled Resid
0	10	1.21	1.2	0.0822	0.0829	0.395
406	9	1.21	1.2	0.096	0.0829	0.374
825	10	1.18	1.2	0.0791	0.0829	-0.75
1643	10	1.25	1.25	0.111	0.0829	-0.00000196
3274	10	1.34	1.33	0.0538	0.0829	0.381
6369	10	1.32	1.33	0.0885	0.0829	-0.381

Likelihoods of Interest

Model	Log(likelihood)	# Param's	AIC
A1	117.992549	7	-221.985098
A2	120.600135	12	-217.20027
A3	117.992549	7	-221.985098
fitted	117.41244	4	-226.82488
R	105.528775	2	-207.05755

Tests of Interest

Test	- 2*log(Likelihood Ratio)	Test df	p-value
Test 1	30.1427	10	0.0008118
Test 2	5.21517	5	0.3902
Test 3	5.21517	5	0.3902
Test 4	1.16022	3	0.7626

Table C-10. Summary of BMD modeling results for relative kidney weight in male F344 rats exposed to *tert*-butanol via inhalation for 6 hr/d, 5d/wk for 13 weeks (NTP, 1997); BMR = 10% relative deviation from the mean.

Model ^a	Goodness of fit		BMC _{10RD} (mg/m ³)	BMCL _{10RD} (mg/m ³)	Basis for model selection
	<i>p</i> -value	AIC			
Exponential (M2) Exponential (M3) ^b	0.168	-141.06	6356	4923	The linear model is selected on the basis of lowest AIC.
Exponential (M4)	0.169	-140.46	5973	3386	
Exponential (M5)	0.560	-142.35	error ^c	0	
Hill	0.612	-142.53	error ^c	error ^c	
Power^d Polynomial 5^{oe} Polynomial 4^{of} Polynomial 3^{og} Polynomial 2^{oh} Linear	0.181	-141.25	6309	4821	

^a Constant variance case presented (BMCS Test 2 *p*-value = 0.165), selected model in bold; scaled residuals for selected model for doses 0, 406, 825, 1643, 3274, and 6369 mg/m³ were 0.181, 0.282, -1.42, -0.102, 1.81, and -0.736, respectively.

^b For the Exponential (M3) model, the estimate of *d* was 1 (boundary). The models in this row reduced to the Exponential (M2) model.

^c BMC or BMCL computation failed for this model.

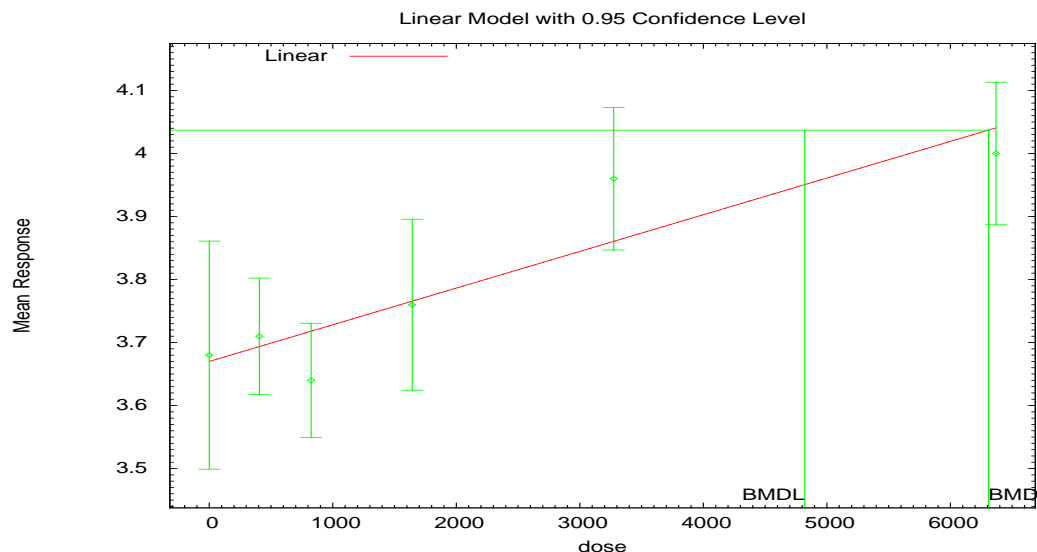
^d For the Power model, the power parameter estimate was 1. The models in this row reduced to the Linear model.

^e For the Polynomial 5° model, the *b*₅, *b*₄, and *b*₃ coefficient estimates were 0 (boundary of parameters space). The models in this row reduced to the Polynomial 2° model. For the Polynomial 5° model, the beta coefficient estimates were 0 (boundary of parameters space). The models in this row reduced to the Linear model.

^f For the Polynomial 4° model, the *b*₄ and *b*₃ coefficient estimates were 0 (boundary of parameters space). The models in this row reduced to the Polynomial 2° model. For the Polynomial 4° model, the *b*₄, *b*₃, and *b*₂ coefficient estimates were 0 (boundary of parameters space). The models in this row reduced to the Linear model.

^g For the Polynomial 3° model, the *b*₃ coefficient estimates was 0 (boundary of parameters space). The models in this row reduced to the Polynomial 2° model. For the Polynomial 3° model, the *b*₃ and *b*₂ coefficient estimates were 0 (boundary of parameters space). The models in this row reduced to the Linear model.

^h For the Polynomial 2° model, the *b*₂ coefficient estimate was 0 (boundary of parameters space). The models in this row reduced to the Linear model.



10:24 04/30 2014

Figure C-8. Plot of mean response by dose, with fitted curve for selected model; dose shown in mg/m^3 .

Polynomial Model. (Version: 2.16; Date: 05/26/2010)

The form of the response function is: $Y[\text{dose}] = \text{beta}_0 + \text{beta}_1 * \text{dose}$

A constant variance model is fit

Benchmark Dose Computation.

BMR = 10% Relative risk

BMD = 6308.98

BMDL at the 95% confidence level = 4820.9

Parameter Estimates

Variable	Estimate	Default Initial Parameter Values
alpha	0.0303258	0.0303618
rho	n/a	0
beta_0	3.67004	3.67051
beta_1	0.0000581717	0.000058076

Table of Data and Estimated Values of Interest

Dose	N	Obs Mean	Est Mean	Obs Std Dev	Est Std Dev	Scaled Resid
0	10	3.68	3.67	0.253	0.174	0.181
406	9	3.71	3.69	0.12	0.174	0.282
825	10	3.64	3.72	0.126	0.174	-1.42
1643	10	3.76	3.77	0.19	0.174	-0.102

Supplemental Information—tert Butanol

3274	10	3.96	3.86	0.158	0.174	1.81
6369	10	4	4.04	0.158	0.174	-0.736

Likelihoods of Interest

Model	Log(likelihood)	# Param's	AIC
A1	76.753535	7	-139.507071
A2	80.677068	12	-137.354137
A3	76.753535	7	-139.507071
fitted	73.624808	3	-141.249616
R	60.931962	2	-117.863925

Tests of Interest

Test	- 2*log(Likelihood Ratio)	Test df	p-value
Test 1	39.4902	10	<0.0001
Test 2	7.84707	5	0.1649
Test 3	7.84707	5	0.1649
Test 4	6.25745	4	0.1807

Table C-11. Summary of BMD modeling results for absolute kidney weight in female F344 rats exposed to *tert*-butanol via inhalation for 6 hr/d, 5d/wk for 13 weeks (NTP, 1997); BMR = 10% relative deviation from the mean.

Model ^a	Goodness of fit		BMC _{10RD} (mg/m ³)	BMCL _{10RD} (mg/m ³)	Basis for model selection
	<i>p</i> -value	AIC			
Exponential (M2) Exponential (M3) ^b	0.0378	-261.52	14500	7713	No model adequately fit the data.
Exponential (M4)	0.533	-267.48	error ^c	0	
Exponential (M5)	0.374	-265.71	error ^c	0	
Hill	0.227	-265.57	error ^c	error ^c	
Power	0.0392	-261.61	14673	7678	
Polynomial 3 ^{°d} Polynomial 2 ^{°e} Linear	0.0274	-261.61	14673	7678	
Polynomial 5 [°]	0.0274	-261.61	14673	7569	
Polynomial 4 [°]	0.0274	-261.61	14673	7674	

^a Modeled variance case presented (BMDS Test 2 *p*-value = 1.90E-04, BMDS Test 3 *p*-value = 0.374), no model was selected as a best-fitting model.

^b For the Exponential (M3) model, the estimate of *d* was 1 (boundary). The models in this row reduced to the Exponential (M2) model.

^c BMC or BMCL computation failed for this model.

^d For the Polynomial 3[°] model, the b3 coefficient estimates was 0 (boundary of parameters space). The models in this row reduced to the Polynomial 2[°] model. For the Polynomial 3[°] model, the b3 and b2 coefficient estimates were 0 (boundary of parameters space). The models in this row reduced to the Linear model.

^e For the Polynomial 2[°] model, the b2 coefficient estimate was 0 (boundary of parameters space). The models in this row reduced to the Linear model.

Table C-12. Summary of BMD modeling results for relative kidney weight in female F344 rats exposed to tert-butanol via inhalation for 6 hrs/d, 5d/wk for 13 weeks (NTP, 1997); BMR = 10% relative deviation from the mean.

Model ^a	Goodness of fit		BMC _{10RD} (mg/m ³)	BMCL _{10RD} (mg/m ³)	Basis for model selection
	p-value	AIC			
Exponential (M2) Exponential (M3) ^b	0.813	-125.14	6859	5476	No model adequately fit the data.
Exponential (M4) ^c	0.660	-123.12	6846	4832	
Exponential (M5) ^d	0.660	-123.12	6846	4832	
Hill	0.00189	-123.12	6845	5380	
Power	0.809	-125.12	6846	5389	
Polynomial 3°	0.00210	-123.34	6853	5439	
Polynomial 2°	0.00191	-123.14	6865	5393	
Linear	0.00488	-125.12	6846	5389	
Polynomial 5°	0.00238	-123.61	6762	5504	
Polynomial 4°	0.00228	-123.51	6807	5480	

^a Modeled variance case presented (BMDS Test 2 p-value = <0.0001, BMDS Test 3 p-value = 0.00105), no model was selected as a best-fitting model.

^b For the Exponential (M3) model, the estimate of d was 1 (boundary). The models in this row reduced to the Exponential (M2) model.

^c The Exponential (M4) model may appear equivalent to the Exponential (M5) model, however differences exist in digits not displayed in the table.

^d The Exponential (M5) model may appear equivalent to the Exponential (M4) model, however differences exist in digits not displayed in the table.

C.1.2. Cancer Endpoints

For each endpoint, multistage models were fitted to the data using the maximum likelihood method. Each model was tested for goodness-of-fit using a chi-square goodness-of-fit test (χ^2 p-value < 0.05¹ indicates lack of fit). Other factors were used to assess model fit, such as scaled residuals, visual fit, and adequacy of fit in the low dose region and near the BMR.

For each endpoint, the BMDL estimate (95% lower confidence limit on the BMD, as estimated by the profile likelihood method) and AIC value were used to select a best-fit model from among the models exhibiting adequate fit. If the BMDL estimates were “sufficiently close,” that is, differed by more than 3-fold, the model selected was the one that yielded the lowest AIC value. If the BMDL estimates were not sufficiently close, the lowest BMDL was selected as the POD. For the

¹ A significance level of 0.05 is used for selecting cancer models because the model family (multistage) is selected a priori (U.S. EPA, 2000).

[NTP \(1995\)](#) and [Hard et al. \(2011\)](#) data, models were run with all doses included, as well as with the high dose dropped. Dropping the high dose resulted in a better fit to the data. Including the high dose caused the model to overestimate the control.

Table C-13. Cancer endpoints selected for dose-response modeling for *tert*-butanol

Endpoint/Study	Species / Sex	Doses and Effect Data				
		Dose (mg/kg-d)	0	90	200	420
Renal tubule adenoma or carcinoma NTP (1995)	Rat (F344) / Male	Incidence / Total	8 / 50	13 / 50	19 / 50	13 / 50
		Dose (PBPK, mg/L)	0	4.6945	12.6177	40.7135
Renal tubule adenoma or carcinoma NTP (1995)	Rat (F344) / Male	Incidence / Total	8 / 50	13 / 50	19 / 50	13 / 50
		Dose (PBPK, mg/hr)	0	0.7992	1.7462	3.4712
Renal tubule adenoma or carcinoma NTP (1995)	Rat (F344) / Male	Incidence / Total	8 / 50	13 / 50	19 / 50	13 / 50
		Dose (mg/kg-d)	0	90	200	420
Renal tubule adenoma or carcinoma; Hard reanalysis NTP (1995);Hard et al. (2011)	Rat (F344) / Male	Incidence / Total	4 / 50	13 / 50	18 / 50	12 / 50
		Dose (PBPK, mg/L)	0	4.6945	12.6177	40.7135
Renal tubule adenoma or carcinoma; Hard reanalysis NTP (1995);Hard et al. (2011)	Rat (F344) / Male	Incidence / Total	4 / 50	13 / 50	18 / 50	12 / 50
		Dose (PBPK, mg/hr)	0	0.7992	1.7462	3.4712
Renal tubule adenoma or carcinoma; Hard reanalysis NTP (1995);Hard et al. (2011)	Rat (F344) / Male	Incidence / Total	4 / 50	13 / 50	18 / 50	12 / 50
		Dose (mg/kg-d)	0	510	1,020	2,110
Thyroid follicular cell adenoma NTP (1995)	B6C3F ₁ mice / female	Incidence / Total	2 / 58	3 / 60	2 / 59	9 / 59

C.1.2.1. Modeling Results

Below are tables summarizing the modeling results for the cancer endpoints that were modeled. For the multistage models, the coefficients were restricted to be non-negative (beta values ≥ 0).

Table C-14. Summary of BMD modeling results for renal tubule adenoma or carcinoma in male F344 rats exposed to *tert*-butanol in drinking water for 2 years modeled with administered dose units and including all dose groups (NTP, 1995); BMR = 10% extra risk.

Model ^a	Goodness of fit			BMD _{10Pct} (mg/kg-d)	BMDL _{10Pct} (mg/kg-d)	Basis for model selection
	<i>p</i> -value	Scaled residuals	AIC			
Three	0.080	-0.989, 0.288,	233.9	294	118	Multistage 2° is selected as the most parsimonious model of adequate fit.
Two	6	1.719, and -1.010	4			
One	0.080	-0.989, 0.288, 1.719, and -1.010	233.9	294	error ^b	
	6		4			

^a Selected model in bold.

^b BMD or BMDL computation failed for this model.

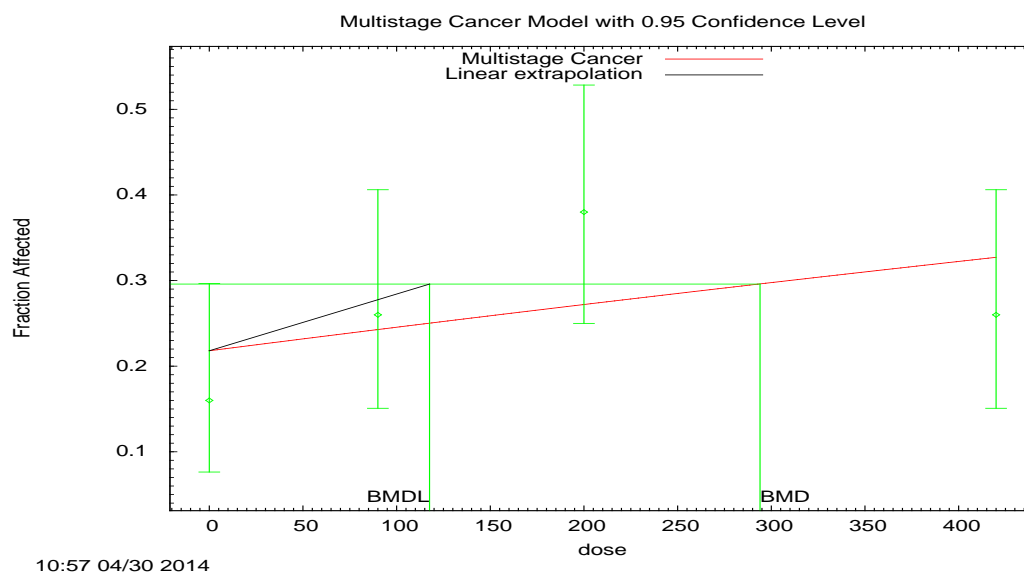


Figure C-9. Plot of incidence rate by dose, with fitted curve for selected model; dose shown in mg/kg-d.

Multistage Cancer Model. (Version: 1.9; Date: 05/26/2010)

The form of the probability function is: $P[\text{response}] = \text{background} + (1 - \text{background}) * [1 - \text{EXP}(-\text{beta1} * \text{dose}^1 - \text{beta2} * \text{dose}^2 \dots)]$

The parameter betas are restricted to be positive

Benchmark Dose Computation.

BMR = 10% Extra risk

BMD = 293.978

BMDL at the 95% confidence level = 117.584

BMDU at the 95% confidence level = 543384000

Taken together, (117.584, 543384000) is a 90% two-sided confidence interval for the BMD

Multistage Cancer Slope Factor = 0.000850453

Parameter Estimates

Variable	Estimate	Default Initial Parameter Values
Background	0.217704	0.2335
Beta(1)	0.000358397	0.000268894
Beta(2)	0	0

Analysis of Deviance Table

Model	Log(likelihood)	# Param's	Deviance	Test d.f.	p-value
Full model	-112.492	4			
Fitted model	-114.97	2	4.95502	2	0.08395
Reduced model	-115.644	1	6.30404	3	0.09772

AIC: = 233.94

Goodness of Fit Table

Dose	Est. Prob.	Expected	Observed	Size	Scaled Resid
0	0.2177	10.885	8	50	-0.989
90	0.2425	12.127	13	50	0.288
200	0.2718	13.591	19	50	1.719
420	0.327	16.351	13	50	-1.01

$\chi^2 = 5.04$ d.f = 2 P-value = 0.0806

Table C-15. Summary of BMD modeling results for renal tubule adenoma or carcinoma in male F344 rats exposed to *tert*-butanol in drinking water for 2 years modeled with administered dose units and excluding high-dose group (NTP, 1995); BMR = 10% extra risk.

Model ^a	Goodness of fit			BMD _{10Pct} (mg/kg-d)	BMDL _{10Pct} (mg/kg-d)	Basis for model selection
	p-value	Scaled residuals	AIC			
Two	N/A ^b	0.000, -0.000, and -0.000	173.68	75.6	41.6	Multistage 1° was selected as the only adequately-fitting model available
One	0.924	0.031, -0.078, and 0.045	171.69	70.1	41.6	

^a Selected model in bold.

^b No available degrees of freedom to calculate a goodness of fit value.

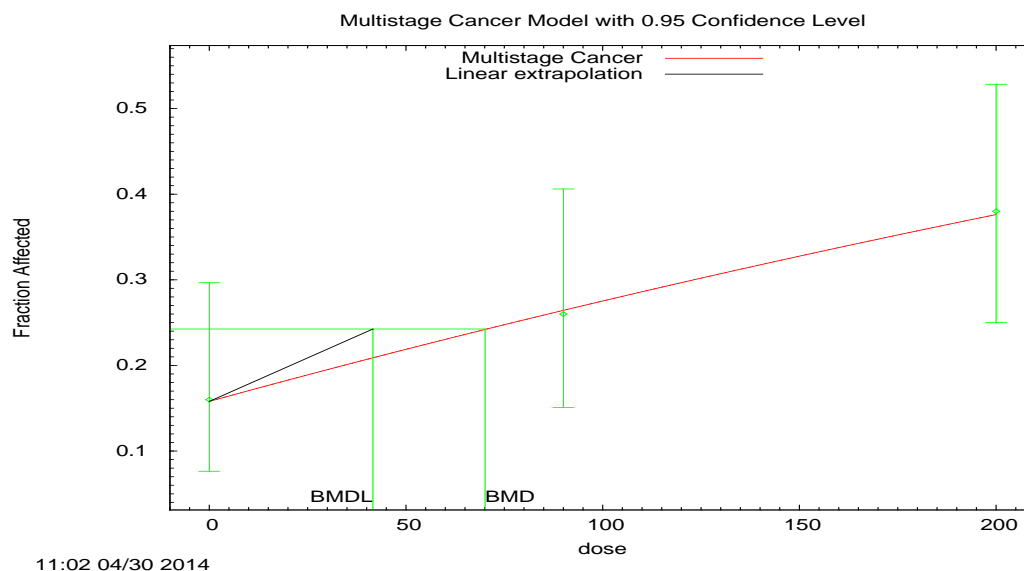


Figure C-10. Plot of incidence rate by dose, with fitted curve for selected model; dose shown in mg/kg-d.

Multistage Cancer Model. (Version: 1.9; Date: 05/26/2010)

The form of the probability function is: $P[\text{response}] = \text{background} + (1 - \text{background}) * [1 - \text{EXP}(-\text{beta1} * \text{dose}^1 - \text{beta2} * \text{dose}^2 \dots)]$

The parameter betas are restricted to be positive

Benchmark Dose Computation.

BMR = 10% Extra risk

BMD = 70.1068

BMDL at the 95% confidence level = 41.5902

BMDU at the 95% confidence level = 203.311

Taken together, (41.5902, 203.311) is a 90% two-sided confidence interval for the BMD

Multistage Cancer Slope Factor = 0.00240441

Parameter Estimates

Variable	Estimate	Default Initial Parameter Values
Background	0.158399	0.156954
Beta(1)	0.00150286	0.0015217

Analysis of Deviance Table

Model	Log(likelihood)	# Param's	Deviance	Test d.f.	p-value
Full model	-83.8395	3			
Fitted model	-83.8441	2	0.00913685	1	0.9238
Reduced model	-86.9873	1	6.29546	2	0.04295

AIC: = 171.688

Goodness of Fit Table

Dose	Est. Prob.	Expected	Observed	Size	Scaled Resid
0	0.1584	7.92	8	50	0.031
90	0.2649	13.243	13	50	-0.078
200	0.3769	18.844	19	50	0.045

Chi^2 = 0.01 d.f = 1 P-value = 0.9239

Table C-16. Summary of BMD modeling results for renal tubule adenoma or carcinoma in male F344 rats exposed to *tert*-butanol in drinking water for 2 years modeled with PBPK (*tert*-butanol, mg/L) dose units and including all dose groups ([NTP, 1995](#)); BMR = 10% extra risk.

Model ^a	Goodness of fit			BMD _{10Pct} (mg/L)	BMDL _{10Pct} (mg/L)	Basis for model selection
	<i>p</i> -value	Scaled residuals	AIC			
Three	0.051	-1.373, 0.155,	234.8	51.8	13.9	Multistage 1° was selected as the most parsimonious model of adequate fit.
Two	8	1.889, and -0.668	3			
One						

^a Selected model in bold.

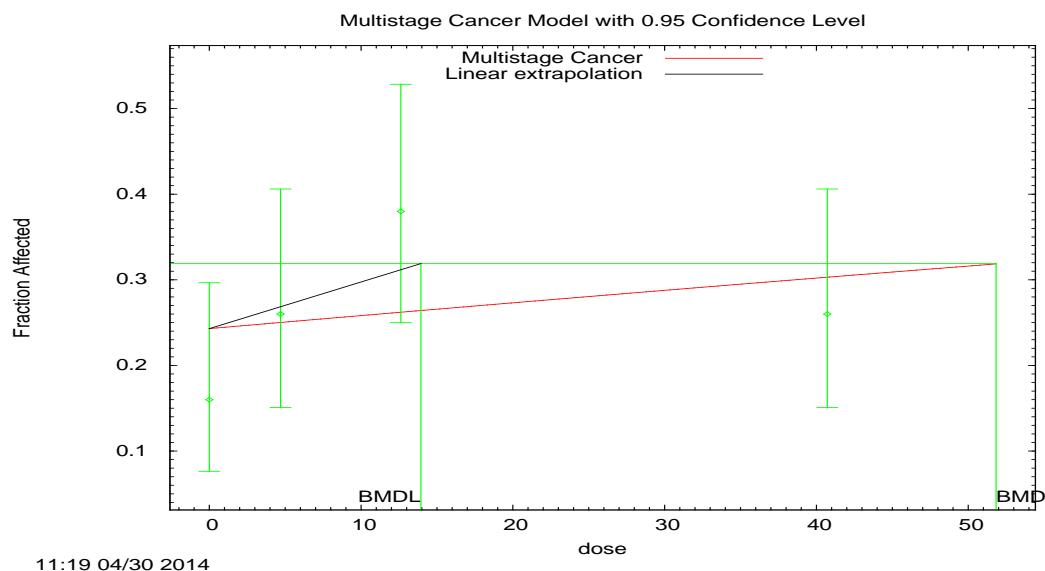


Figure C-11. Plot of incidence rate by dose, with fitted curve for selected model; dose shown in mg/L.

Multistage Cancer Model. (Version: 1.9; Date: 05/26/2010)

The form of the probability function is: $P[\text{response}] = \text{background} + (1 - \text{background}) * [1 - \text{EXP}(-\text{beta1} * \text{dose}^1 - \text{beta2} * \text{dose}^2 \dots)]$

The parameter betas are restricted to be positive

Benchmark Dose Computation.

BMR = 10% Extra risk

BMD = 51.8357

BMDL at the 95% confidence level = 13.9404

BMDU at the 95% confidence level = error

Taken together, (13.9404, error) is a 90% two-sided confidence interval for the BMD

Multistage Cancer Slope Factor = error

Parameter Estimates

Variable	Estimate	Default Initial Parameter Values
Background	0.243327	0.253053
Beta(1)	0.00203259	0.00150893

Analysis of Deviance Table

Model	Log(likelihood)	# Param's	Deviance	Test d.f.	p-value
Full model	-112.492	4			
Fitted model	-115.417	2	5.84883	2	0.0537
Reduced model	-115.644	1	6.30404	3	0.09772

AIC: = 234.834

Goodness of Fit Table

Dose	Est. Prob.	Expected	Observed	Size	Scaled Resid
0	0.2433	12.166	8	50	-1.373
4.6945	0.2505	12.526	13	50	0.155
12.6177	0.2625	13.124	19	50	1.889
40.7135	0.3034	15.171	13	50	-0.668

$\chi^2 = 5.92$ d.f = 2 P-value = 0.0518

Table C-17. Summary of BMD modeling results for renal tubule adenoma or carcinoma in male F344 rats exposed to *tert*-butanol in drinking water for 2 years modeled with PBPK (*tert*-butanol, mg/L) dose units and excluding high-dose group (NTP, 1995); BMR = 10% extra risk.

Model ^a	Goodness of fit			BMD _{10Pct} (mg/L)	BMDL _{10Pct} (mg/L)	Basis for model selection
	<i>p</i> -value	Scaled residuals	AIC			
Two One	0.891	-0.054, 0.113, and -0.057	171.70	4.33	2.54	Multistage 1° was selected as the most parsimonious model of adequate fit.

^a Selected model in bold.

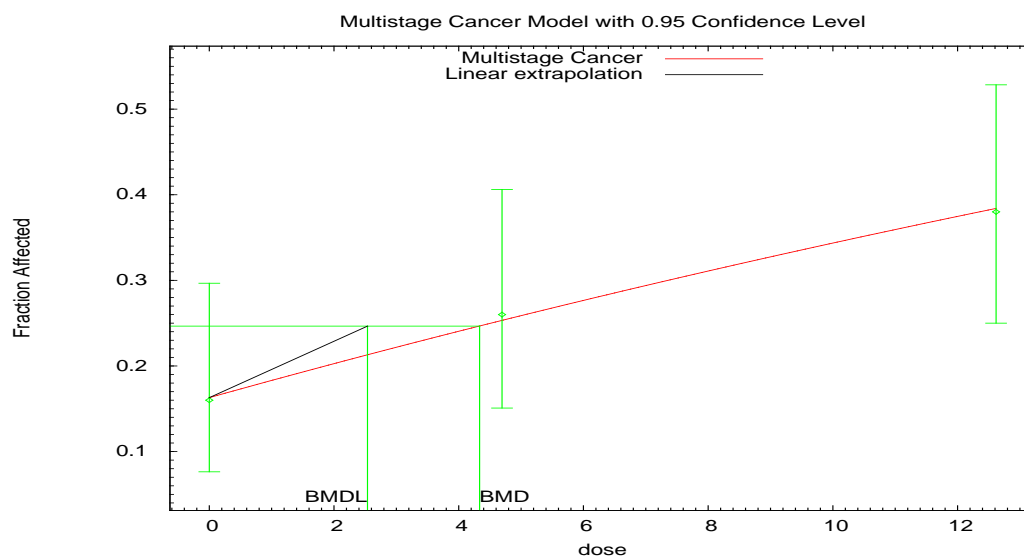


Figure C-12. Plot of incidence rate by dose, with fitted curve for selected model; dose shown in mg/L.

Multistage Cancer Model. (Version: 1.9; Date: 05/26/2010)

The form of the probability function is: $P[\text{response}] = \text{background} + (1 - \text{background}) * [1 - \text{EXP}(-\text{beta1} * \text{dose}^1 - \text{beta2} * \text{dose}^2 \dots)]$

The parameter betas are restricted to be positive

Benchmark Dose Computation.

BMR = 10% Extra risk

BMD = 4.33496

BMDL at the 95% confidence level = 2.53714

BMDU at the 95% confidence level = 12.8097

Taken together, (2.53714, 12.8097) is a 90% two-sided confidence interval for the BMD

Multistage Cancer Slope Factor = 0.0394144

Parameter Estimates

Variable	Estimate	Default Initial Parameter Values
Background	0.162798	0.164724
Beta(1)	0.0243048	0.0238858

Analysis of Deviance Table

Model	Log(likelihood)	# Param's	Deviance	Test d.f.	p-value
Full model	-83.8395	3			
Fitted model	-83.8489	2	0.0187339	1	0.8911
Reduced model	-86.9873	1	6.29546	2	0.04295

AIC: = 171.698

Goodness of Fit Table

Dose	Est. Prob.	Expected	Observed	Size	Scaled Resid
0	0.1628	8.14	8	50	-0.054
4.6945	0.2531	12.654	13	50	0.113
12.6177	0.3839	19.195	19	50	-0.057

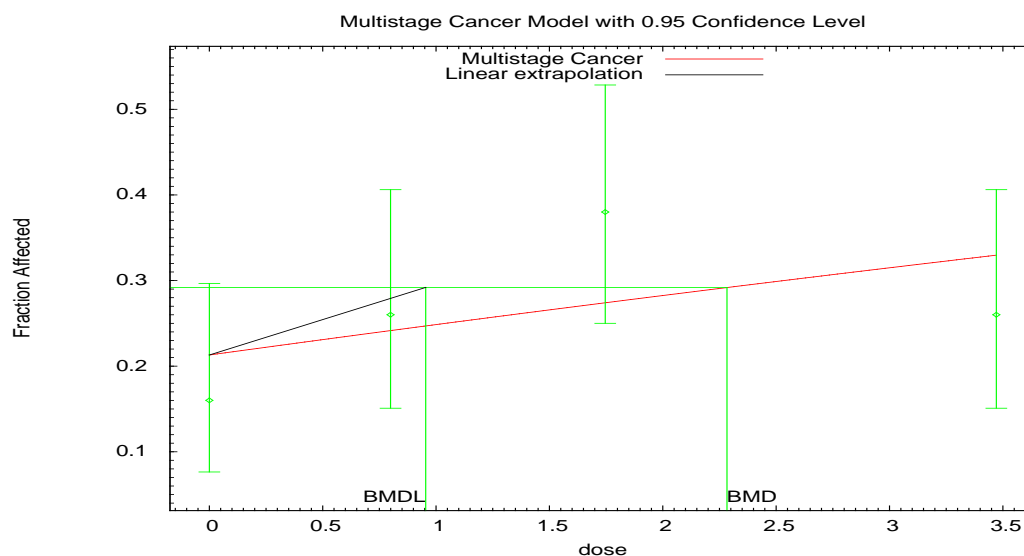
$\chi^2 = 0.02$ d.f = 1 P-value = 0.891

Table C-18. Summary of BMD modeling results for renal tubule adenoma or carcinoma in male F344 rats exposed to *tert*-butanol in drinking water for 2 years modeled with PBPK (metabolized, mg/hr) dose units and including all dose groups ([NTP, 1995](#)); BMR = 10% extra risk.

Model ^a	Goodness of fit			BMD _{10Pct} (mg/hr)	BMDL _{10Pct} (mg/hr)	Basis for model selection
	<i>p</i> -value	Scaled residuals	AIC			
Three Two One	0.088 5	-0.920, 0.301, 1.677, and -1.049	233.7 6	2.28	0.954	Multistage 1° was selected as the most parsimonious model of adequate fit.

^a Selected model in bold.

Data from NTP1995



11:22 04/30 2014

Figure C-13. Plot of incidence rate by dose, with fitted curve for selected model; dose shown in mg/hr.

Multistage Cancer Model. (Version: 1.9; Date: 05/26/2010)

The form of the probability function is: $P[\text{response}] = \text{background} + (1 - \text{background}) * [1 - \text{EXP}(-\text{beta1} * \text{dose}^1 - \text{beta2} * \text{dose}^2 \dots)]$

The parameter betas are restricted to be positive

Benchmark Dose Computation.

BMR = 10% Extra risk

BMD = 2.28299

BMDL at the 95% confidence level = 0.95436

BMDU at the 95% confidence level = error

Taken together, (0.95436, error) is a 90% two-sided confidence interval for the BMD

Multistage Cancer Slope Factor = error

Parameter Estimates

Variable	Estimate	Default Initial Parameter Values
Background	0.21328	0.229822
Beta(1)	0.0461502	0.0349139

Analysis of Deviance Table

Model	Log(likelihood)	# Param's	Deviance	Test d.f.	p-value
Full model	-112.492	4			
Fitted model	-114.879	2	4.77309	2	0.09195
Reduced model	-115.644	1	6.30404	3	0.09772

AIC: = 233.758

Goodness of Fit Table

Dose	Est. Prob.	Expected	Observed	Size	Scaled Resid
0	0.2133	10.664	8	50	-0.92
0.7992	0.2418	12.088	13	50	0.301
1.7462	0.2742	13.71	19	50	1.677
3.4712	0.3297	16.487	13	50	-1.049

$\chi^2 = 4.85$ d.f = 2 P-value = 0.0885

Table C-19. Summary of BMD modeling results for renal tubule adenoma or carcinoma in male F344 rats exposed to *tert*-butanol in drinking water for 2 years modeled with PBPK (metabolized, mg/hr) dose units and excluding high-dose group ([NTP, 1995](#)); BMR = 10% extra risk.

Model ^a	Goodness of fit			BMD _{10Pct} (mg/hr)	BMDL _{10Pct} (mg/hr)	Basis for model selection
	p-value	Scaled residuals	AIC			
Two	N/A ^b	-0.000, -0.000, and -0.000	173.68	0.673	0.365	Multistage 1° was selected on the basis of lowest AIC.
One	0.906	0.037, -0.096, and 0.057	171.69	0.614	0.364	

^a Selected model in bold.

^b No available degrees of freedom to calculate a goodness of fit value.

Data from NTP1995

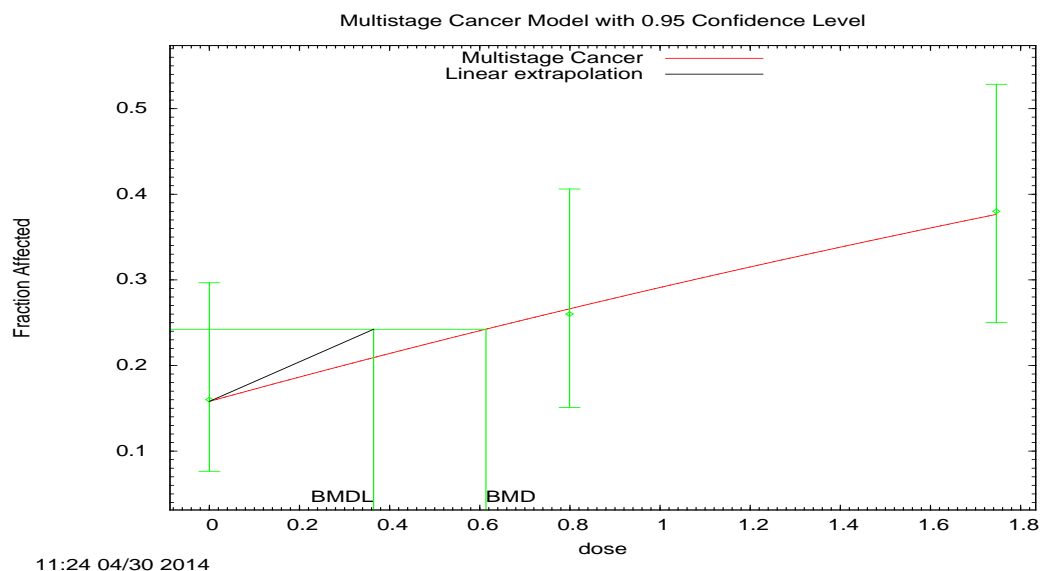


Figure C-14. Plot of incidence rate by dose, with fitted curve for selected model; dose shown in mg/hr.

Multistage Cancer Model. (Version: 1.9; Date: 05/26/2010)

The form of the probability function is: $P[\text{response}] = \text{background} + (1 - \text{background}) * [1 - \text{EXP}(-\text{beta1} * \text{dose}^1 - \text{beta2} * \text{dose}^2 \dots)]$

The parameter betas are restricted to be positive

Benchmark Dose Computation.

BMR = 10% Extra risk

BMD = 0.613798

BMDL at the 95% confidence level = 0.364494

BMDU at the 95% confidence level = 1.77845

Taken together, (0.364494, 1.77845) is a 90% two-sided confidence interval for the BMD

Multistage Cancer Slope Factor = 0.274353

Parameter Estimates

Variable	Estimate	Default Initial Parameter Values
Background	0.158068	0.156284
Beta(1)	0.171653	0.174305

Analysis of Deviance Table

Model	Log(likelihood)	# Param's	Deviance	Test d.f.	p-value
Full model	-83.8395	3			
Fitted model	-83.8465	2	0.0138544	1	0.9063
Reduced model	-86.9873	1	6.29546	2	0.04295

AIC: = 171.693

Goodness of Fit Table

Dose	Est. Prob.	Expected	Observed	Size	Scaled Resid
0	0.1581	7.903	8	50	0.037
0.7992	0.266	13.3	13	50	-0.096
1.7462	0.3761	18.806	19	50	0.057

Chi^2 = 0.01 d.f = 1 P-value = 0.9064

Table C-20. Summary of BMD modeling results for renal tubule adenoma or carcinoma in male F344 rats exposed to *tert*-butanol in drinking water for 2 years modeled with administered dose units and including all dose groups; reanalyzed data ([Hard et al., 2011](#); [NTP, 1995](#)); BMR = 10% extra risk.

Model ^a	Goodness of fit			BMD _{10Pct} (mg/kg-d)	BMDL _{10Pct} (mg/kg-d)	Basis for model selection
	<i>p</i> -value	Scaled residuals	AIC			
Three Two One	0.011 7	-1.476, 1.100, 1.855, and -1.435	218.6 8	184	94.8	No model fit the data.

^a No model was selected as a best-fitting model.

Table C-21. Summary of BMD modeling results for renal tubule adenoma or carcinoma in male F344 rats exposed to *tert*-butanol in drinking water for 2 years modeled with administered dose units and excluding high-dose group; re-analyzed data ([Hard et al., 2011](#); [NTP, 1995](#)); BMR = 10% extra risk.

Model ^a	Goodness of fit			BMD _{10Pct} (mg/kg-d)	BMDL _{10Pct} (mg/kg-d)	Basis for model selection
	<i>p</i> -value	Scaled residuals	AIC			
Two One	0.572	-0.141, 0.461, and -0.296	154.84	54.2	36.3	Multistage 1° was selected as the most parsimonious model of adequate fit.

^a Selected model in bold.

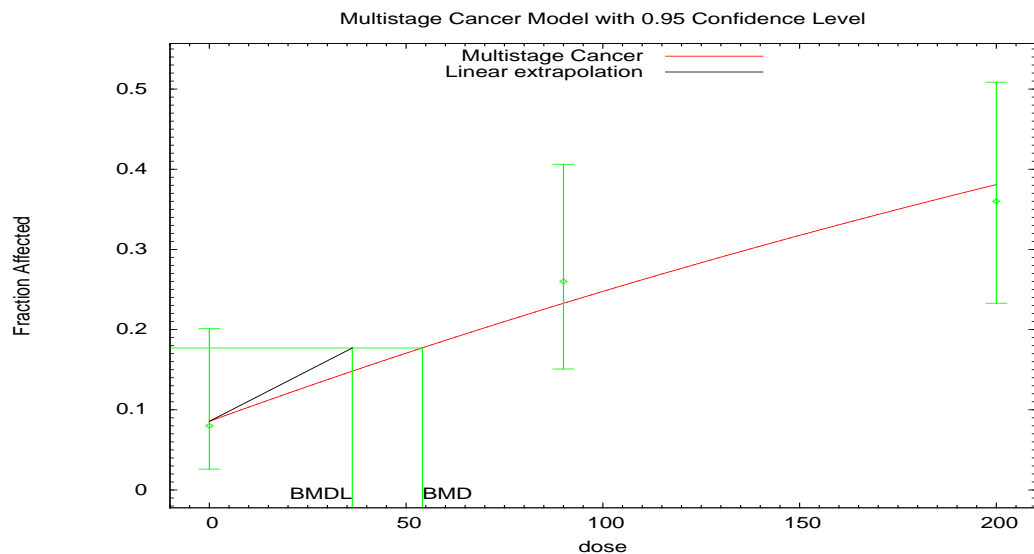


Figure C-15. Plot of incidence rate by dose, with fitted curve for selected model; dose shown in mg/kg-d.

Multistage Cancer Model. (Version: 1.9; Date: 05/26/2010)

The form of the probability function is: $P[\text{response}] = \text{background} + (1 - \text{background}) * [1 - \text{EXP}(-\beta_1 * \text{dose} - \beta_2 * \text{dose}^2)]$

The parameter betas are restricted to be positive

Benchmark Dose Computation.

BMR = 10% Extra risk

BMD = 54.1642

BMDL at the 95% confidence level = 36.3321

BMDU at the 95% confidence level = 101.125

Taken together, (36.3321, 101.125) is a 90% two-sided confidence interval for the BMD

Multistage Cancer Slope Factor = 0.00275239

Parameter Estimates

Variable	Estimate	Default Initial Parameter Values
Background	0.0855815	0.0981146
Beta(1)	0.00194521	0.00179645

Analysis of Deviance Table

Model	Log(likelihood)	# Param's	Deviance	Test d.f.	p-value
Full model	-75.2622	3			
Fitted model	-75.4201	2	0.315716	1	0.5742
Reduced model	-81.4909	1	12.4574	2	0.001972

AIC: = 154.84

Goodness of Fit Table

Dose	Est. Prob.	Expected	Observed	Size	Scaled Resid
0	0.0856	4.279	4	50	-0.141
90	0.2324	11.622	13	50	0.461
200	0.3803	19.015	18	50	-0.296

Chi² = 0.32 d.f = 1 P-value = 0.5715

Table C-22. Summary of BMD modeling results for renal tubule adenoma or carcinoma in male F344 rats exposed to *tert*-butanol in drinking water for 2 years modeled with PBPK (*tert*-butanol, mg/L) dose units and including all dose groups; reanalyzed data ([Hard et al., 2011](#); [NTP, 1995](#)); BMR = 10% extra risk.

Model ^a	Goodness of fit			BMD _{10Pct} (mg/L)	BMDL _{10Pct} (mg/L)	Basis for model selection
	<i>p</i> -value	Scaled residuals	AIC			
Three Two One	0.0048	-2.089, 0.864, 2.165, and -0.929	220.82	31.4	11.7	No model fit the data.

^a No model was selected as a best-fitting model.

Table C-23. Summary of BMD modeling results for renal tubule adenoma or carcinoma in male F344 rats exposed to *tert*-butanol in drinking water for 2 years modeled with PBPK (*tert*-butanol, mg/L) dose units and excluding high-dose group; reanalyzed data ([Hard et al., 2011](#); [NTP, 1995](#)); BMR = 10% extra risk.

Model ^a	Goodness of fit			BMD _{10Pct} (mg/L)	BMDL _{10Pct} (mg/L)	Basis for model selection
	<i>p</i> -value	Scaled residuals	AIC			
Two One	0.364	-0.285, 0.750, and -0.424	155.33	3.35	2.21	Multistage 1° was selected as the most parsimonious model of adequate fit.

^a Selected model in bold.

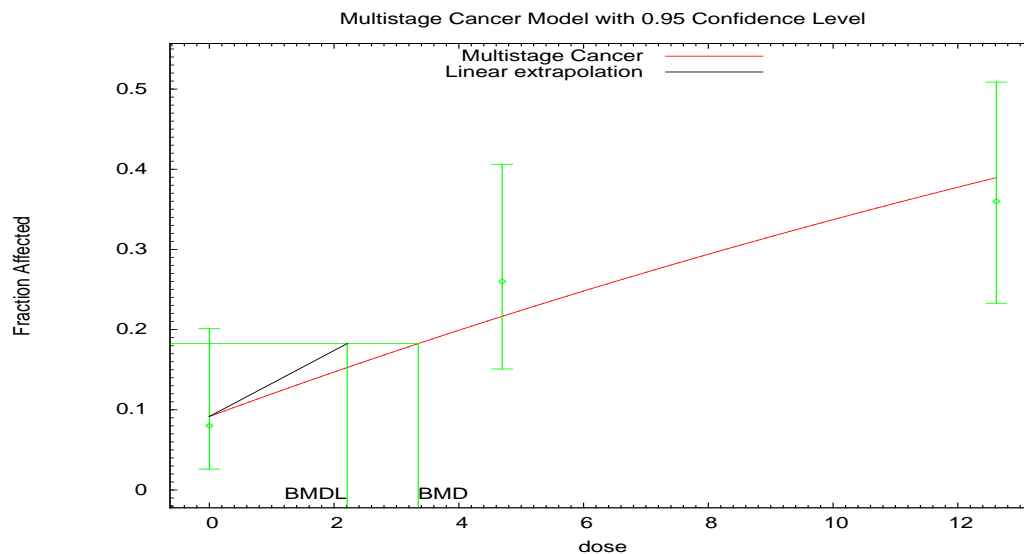


Figure C-16. Plot of incidence rate by dose, with fitted curve for selected model; dose shown in mg/L.

Multistage Cancer Model. (Version: 1.9; Date: 05/26/2010)

The form of the probability function is: $P[\text{response}] = \text{background} + (1 - \text{background}) * [1 - \text{EXP}(-\beta_1 \cdot \text{dose} - \beta_2 \cdot \text{dose}^2)]$

The parameter betas are restricted to be positive

Benchmark Dose Computation.

BMR = 10% Extra risk

BMD = 3.34903

BMDL at the 95% confidence level = 2.20865

BMDU at the 95% confidence level = 6.49702

Taken together, (2.20865, 6.49702) is a 90% two-sided confidence interval for the BMD

Multistage Cancer Slope Factor = 0.0452765

Parameter Estimates

Variable	Estimate	Default Initial Parameter Values
Background	0.0916116	0.110649
Beta(1)	0.03146	0.0276674

Analysis of Deviance Table

Model	Log(likelihood)	# Param's	Deviance	Test d.f.	p-value
Full model	-75.2622	3			
Fitted model	-75.664	2	0.803466	1	0.3701
Reduced model	-81.4909	1	12.4574	2	0.001972

AIC: = 155.328

Goodness of Fit Table

Dose	Est. Prob.	Expected	Observed	Size	Scaled Resid
0	0.0916	4.581	4	50	-0.285
4.6945	0.2163	10.817	13	50	0.75
12.6177	0.3892	19.462	18	50	-0.424

Chi² = 0.82 d.f = 1 P-value = 0.3643

Table C-24. Summary of BMD modeling results for renal tubule adenoma or carcinoma in male F344 rats exposed to *tert*-butanol in drinking water for 2 years modeled with PBPK (metabolized, mg/hr) dose units and including all dose groups; reanalyzed data ([Hard et al., 2011](#); [NTP, 1995](#)); BMR = 10% extra risk.

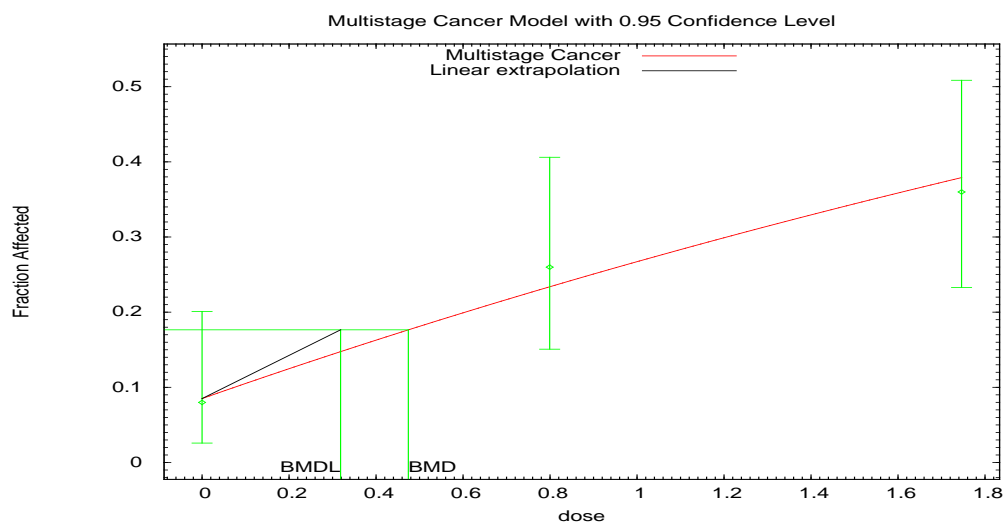
Model ^a	Goodness of fit			BMD _{10Pct} (mg/hr)	BMDL _{10Pct} (mg/hr)	Basis for model selection
	p-value	Scaled residuals	AIC			
Three Two One	0.014 2	-1.367, 1.119, 1.783, and -1.484	218.2 6	1.44	0.770	No model fit the data.

^a No model was selected as a best-fitting model.

Table C-25. Summary of BMD modeling results for renal tubule adenoma or carcinoma in male F344 rats exposed to *tert*-butanol in drinking water for 2 years modeled with PBPK (metabolized, mg/hr) dose units and excluding high-dose group; reanalyzed data ([Hard et al., 2011](#); [NTP, 1995](#)); BMR = 10% extra risk.

Model ^a	Goodness of fit			BMD _{10Pct} (mg/hr)	BMDL _{10Pct} (mg/hr)	Basis for model selection
	p-value	Scaled residuals	AIC			
Two One	0.593	-0.130, 0.435, and -0.281	154.81	0.474	0.319	Multistage 1° was selected as the most parsimonious model of adequate fit.

^a Selected model in bold.



11:33 04/30 2014

Figure C-17. Plot of incidence rate by dose, with fitted curve for selected model; dose shown in mg/hr.

Multistage Cancer Model. (Version: 1.9; Date: 05/26/2010)

The form of the probability function is: $P[\text{response}] = \text{background} + (1 - \text{background}) * [1 - \text{EXP}(-\beta_1 \text{dose} - \beta_2 \text{dose}^2)]$

The parameter betas are restricted to be positive

Benchmark Dose Computation.

BMR = 10% Extra risk

BMD = 0.474241

BMDL at the 95% confidence level = 0.318504

BMDU at the 95% confidence level = 0.882859

Taken together, (0.318504, 0.882859) is a 90% two-sided confidence interval for the BMD

Multistage Cancer Slope Factor = 0.313968

Parameter Estimates

Variable	Estimate	Default Initial Parameter Values
Background	0.0851364	0.0969736
Beta(1)	0.222167	0.206161

Analysis of Deviance Table

Model	Log(likelihood)	# Param's	Deviance	Test d.f.	p-value
Full model	-75.2622	3			
Fitted model	-75.4029	2	0.281435	1	0.5958
Reduced model	-81.4909	1	12.4574	2	0.001972

AIC: = 154.806

Goodness of Fit Table

Dose	Est. Prob.	Expected	Observed	Size	Scaled Resid
0	0.0851	4.257	4	50	-0.13
0.7992	0.234	11.699	13	50	0.435
1.7462	0.3793	18.966	18	50	-0.281

Chi² = 0.29 d.f = 1 P-value = 0.5933

Table C-26. Summary of BMD modeling results for thyroid follicular cell adenomas in female B6C3F1 mice exposed to *tert*-butanol in drinking water for 2 years (NTP, 1995); BMR = 10% extra risk.

Model ^a	Goodness of fit		BMD _{10%} ^c (mg/kg-d)	BMDL _{10%} ^c (mg/kg-d)	Basis for model selection
	p-value	AIC ^b			
Three	0.75	113.665	2002	1437	
Two	0.36	115.402	2186	1217	
One	0.63	114.115	1987	1378	

^a Selected (best-fitting) model shown in boldface type

^b AIC = Akaike Information Criterion

^c Confidence level 0.95

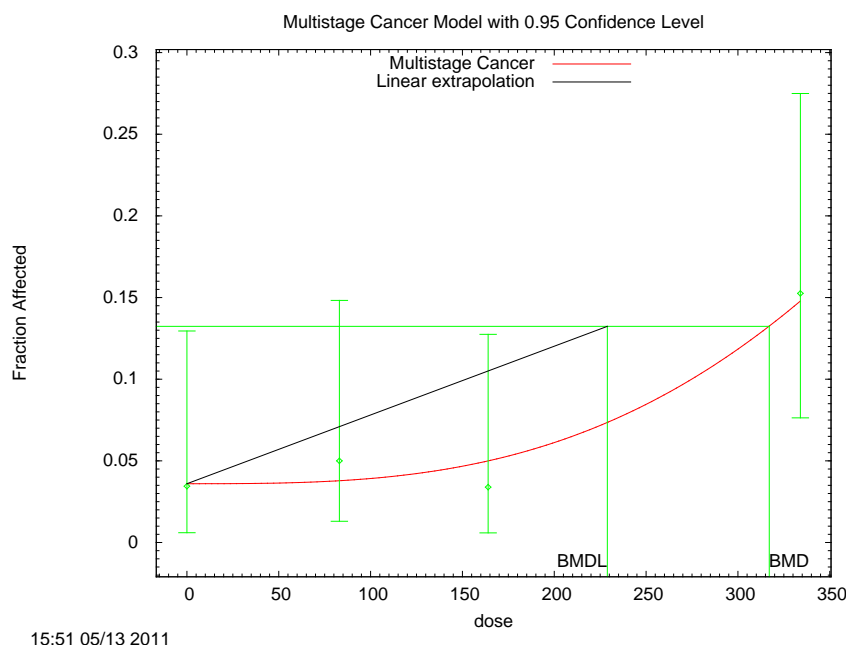


Figure C-18. Plot of mean response by dose, with fitted curve for selected model.

```

=====
Multistage Cancer Model. (Version: 1.9; Date: 05/26/2010)
Input Data File: M:\NCEA tert-butanol\BMD modeling\BMDS Output\29 NTP
1995b_Thyroid folluclar cell andenoma, female mice (HEC)_MultiCanc3_10.(d)
Gnuplot Plotting File: M:\NCEA tert-butanol\BMD modeling\BMDS Output\29 NTP
1995b_Thyroid folluclar cell andenoma, female mice (HEC)_MultiCanc3_10.plt
Fri May 13 15:51:46 2011
=====
[notes]
=====

```

The form of the probability function is:

$$P[\text{response}] = \text{background} + (1 - \text{background}) * [1 - \exp(-\beta_1 \cdot \text{dose} - \beta_2 \cdot \text{dose}^2 - \beta_3 \cdot \text{dose}^3)]$$

The parameter betas are restricted to be positive

Dependent variable = Incidence

Independent variable = Dose

Total number of observations = 4

Total number of records with missing values = 0

Total number of parameters in model = 4

Total number of specified parameters = 0

Degree of polynomial = 3

Maximum number of iterations = 250

Relative Function Convergence has been set to: 1e-008

Parameter Convergence has been set to: 1e-008

Default Initial Parameter Values

Background = 0.0344951

Beta(1) = 0

Beta(2) = 0

Beta(3) = 3.4555e-009

Asymptotic Correlation Matrix of Parameter Estimates

(*** The model parameter(s) -Beta(1) -Beta(2)
have been estimated at a boundary point, or have been specified by the user,
and do not appear in the correlation matrix)

	Background	Beta(3)
Background	1	-0.54
Beta(3)	-0.54	1

Parameter Estimates

Variable	Estimate	95.0% Wald Confidence Interval		
		Std. Err.	Lower Conf. Limit	Upper Conf. Limit
Background	0.0359685	*	*	*
Beta(1)	0	*	*	*
Beta(2)	0	*	*	*
Beta(3)	3.30537e-009	*	*	*

* - Indicates that this value is not calculated.

Analysis of Deviance Table

Model	Log(likelihood)	# Param's	Deviance Test	d.f.	P-value
Full model	-54.5437	4			
Fitted model	-54.8422	2	0.597063	2	0.7419
Reduced model	-58.5048	1	7.92235	3	0.04764

AIC: 113.684

Goodness of Fit

Scaled

This document is a draft for review purposes only and does not constitute Agency policy.

Supplemental Information—tert Butanol

Dose	Est._Prob.	Expected	Observed	Size	Residual
0.0000	0.0360	2.086	2.000	58	-0.061
83.0000	0.0378	2.267	3.000	60	0.496
164.0000	0.0499	2.945	2.000	59	-0.565
334.0000	0.1477	8.713	9.000	59	0.105

Chi^2 = 0.58 d.f. = 2 P-value = 0.7482

Benchmark Dose Computation

Specified effect = 0.1

Risk Type = Extra risk

Confidence level = 0.95

BMD = 317.068

BMDL = 228.888

BMDU = 600.031

Taken together, (228.888, 600.031) is a 90 % two-sided confidence interval for the BMD

Multistage Cancer Slope Factor = 0.000436894

APPENDIX D. SUMMARY OF EXTERNAL PEER REVIEW AND PUBLIC COMMENTS AND EPA'S DISPOSITION

[placeholder]

Additional Appendices:

[appendices can be used to supplement the HI and D-R analysis – the information presented by the appendices will be chemical-specific]

Examples:

- PBPK Modeling of [chemical] and metabolites – detailed methods and results
- Meta-analysis of _____ results from epidemiological studies
- Lifetable analysis and weighted linear regression based on results from [reference]

REFERENCES FOR APPENDICES

- [ACGIH](#) (American Conference of Governmental Industrial Hygienists). (2012). Documentation of the threshold limit values and biological exposure indices tert-Butanol (7th ed.). Cincinnati, OH.
- [Amberg, A; Rosner, E; Dekant, W.](#) (1999). Biotransformation and kinetics of excretion of methyl-tert-butyl ether in rats and humans. *Toxicol Sci* 51: 1-8.
- [Amberg, A; Rosner, E; Dekant, W.](#) (2000). Biotransformation and kinetics of excretion of ethyl tert-butyl ether in rats and humans. *Toxicol Sci* 53: 194-201.
<http://dx.doi.org/10.1093/toxsci/53.2.194>
- [Andersen, ME.](#) (1991). Physiological modelling of organic compounds. *Ann Occup Hyg* 35: 309-321.
- [ARCO](#) (ARCO Chemical Company). (1983). Toxicologist's report on metabolism and pharmacokinetics of radiolabeled TBA 534 tertiary butyl alcohol with cover letter dated 03/24/1994. (8EHQ86940000263). Newton Square, PA.
- [Arslanian, MJ; Pascoe, E; Reinhold, JG.](#) (1971). Rat liver alcohol dehydrogenase. Purification and properties. *Biochem J* 125: 1039-1047.
- [ATSDR](#) (Agency for Toxic Substances and Disease Registry). (1996). Toxicological profile for methyl-tert-butyl ether [ATSDR Tox Profile]. Atlanta, GA: U.S. Department of Health and Human Services, Public Health Service.
<http://www.atsdr.cdc.gov/toxprofiles/tp.asp?id=228&tid=41>
- [Baker, RC; Sorensen, SM; Deitrich, RA.](#) (1982). The in vivo metabolism of tertiary butanol by adult rats. *Alcohol Clin Exp Res* 6: 247-251. <http://dx.doi.org/10.1111/j.1530-0277.1982.tb04970.x>
- [Bernauer, U; Amberg, A; Scheutzw, D; Dekant, W.](#) (1998). Biotransformation of 12C- and 2-13C-labeled methyl tert-butyl ether, ethyl tert-butyl ether, and tert-butyl alcohol in rats: identification of metabolites in urine by 13C nuclear magnetic resonance and gas chromatography/mass spectrometry. *Chem Res Toxicol* 11: 651-658.
<http://dx.doi.org/10.1021/tx970215v>
- [Blancato, JN; Evans, MV; Power, FW; Caldwell, JC.](#) (2007). Development and use of PBPK modeling and the impact of metabolism on variability in dose metrics for the risk assessment of methyl tertiary butyl ether (MTBE). *J Environ Prot Sci* 1: 29-51.
- [Borghoff, S; Murphy, J; Medinsky, M.](#) (1996). Development of physiologically based pharmacokinetic model for methyl tertiary-butyl ether and tertiary-butanol in male Fisher-344 rats. *Fundam Appl Toxicol* 30: 264-275.
<http://dx.doi.org/10.1006/faat.1996.0064>
- [Borghoff, S; Parkinson, H; Leavens, T.](#) (2010). Physiologically based pharmacokinetic rat model for methyl tertiary-butyl ether; comparison of selected dose metrics following various

- 1 MTBE exposure scenarios used for toxicity and carcinogenicity evaluation. Toxicology
- 2 275: 79-91. <http://dx.doi.org/10.1016/j.tox.2010.06.003>
- 3 [Borghoff, SJ; Prescott, JS; Janszen, DB; Wong, BA; Everitt, JL](#). (2001). alpha2u-Globulin
- 4 nephropathy, renal cell proliferation, and dosimetry of inhaled tert-butyl alcohol in male
- 5 and female F-344 rats. Toxicol Sci 61: 176-186.
- 6 [Borghoff, SJ; Short, BG; Swenberg, JA](#). (1990). Biochemical mechanisms and pathobiology of
- 7 alpha 2u-globulin nephropathy [Review]. Annu Rev Pharmacol Toxicol 30: 349-367.
- 8 <http://dx.doi.org/10.1146/annurev.pa.30.040190.002025>
- 9 [Brown, MA; Cornell, BA; Davenport, JB](#). (1977). PERTURBATION OF BIOLOGICAL-MEMBRANES
- 10 WITH TERT-BUTANOL. Seikagaku 49: 1-1.
- 11 [Cederbaum, AI; Cohen, G](#). (1980). Oxidative demethylation of t-butyl alcohol by rat liver
- 12 microsomes. Biochem Biophys Res Commun 97: 730-736.
- 13 [Cederbaum, AI; Qureshi, A; Cohen, G](#). (1983). Production of formaldehyde and acetone by
- 14 hydroxyl-radical generating systems during the metabolism of tertiary butyl alcohol.
- 15 Biochem Pharmacol 32: 3517-3524. [http://dx.doi.org/10.1016/0006-2952\(83\)90297-6](http://dx.doi.org/10.1016/0006-2952(83)90297-6)
- 16 [Dickey, FH; Cleland, GH; Lotz, C](#). (1949). The role of organic peroxides in the induction of
- 17 mutations. PNAS 35: 581-586.
- 18 [Faulkner, T; Hussain, A](#). (1989). The pharmacokinetics of tertiary butanol in C57BL/6J mice. Res
- 19 Comm Chem Pathol Pharmacol 64: 31-39.
- 20 [Faulkner, TP; Wiechart, JD; Hartman, DM; Hussain, AS](#). (1989). The effects of prenatal tertiary
- 21 butanol administration in CBA/J and C57BL/6J mice. Life Sci 45: 1989-1995.
- 22 [FDA](#) (U.S. Food and Drug Administration). (2011a). Indirect food additives: Adjuvants,
- 23 production aids, and sanitizers. Surface lubricants used in the manufacture of metallic
- 24 articles. 21 CFR 178.3910.
- 25 <http://www.accessdata.fda.gov/scripts/cdrh/cfdocs/cfcfr/CFRSearch.cfm?fr=178.3910>
- 26 [FDA](#) (U.S. Food and Drug Administration). (2011b). Indirect food additives: Paper and
- 27 paperboard components. Defoaming agents used in coatings. 21 CFR 176.200.
- 28 <http://www.accessdata.fda.gov/scripts/cdrh/cfdocs/cfcfr/CFRSearch.cfm?fr=176.200>
- 29 [Hard, GC; Bruner, RH; Cohen, SM; Pletcher, JM; Regan, KS](#). (2011). Renal histopathology in
- 30 toxicity and carcinogenicity studies with tert-butyl alcohol administered in drinking
- 31 water to F344 rats: A pathology working group review and re-evaluation. Regul Toxicol
- 32 Pharmacol 59: 430-436. <http://dx.doi.org/10.1016/j.yrtph.2011.01.007>
- 33 [Jimenez, J; Longo, E; Benitez, T](#). (1988). Induction of petite yeast mutants by membrane-active
- 34 agents. Appl Environ Microbiol 54: 3126-3132.
- 35 [Johanson, G; Nihlén, A; Lof, A](#). (1995). Toxicokinetics and acute effects of MTBE and ETBE in
- 36 male volunteers. Toxicol Lett 82/83: 713-718. [http://dx.doi.org/10.1016/0378-](http://dx.doi.org/10.1016/0378-4274(95)03589-3)
- 37 [4274\(95\)03589-3](http://dx.doi.org/10.1016/0378-4274(95)03589-3)
- 38 [Kim, D; Andersen, ME; Pleil, JD; Nylander-French, LA; Prah, JD](#). (2007). Refined PBPK model of
- 39 aggregate exposure to methyl tertiary-butyl ether. Toxicol Lett 169: 222-235.
- 40 <http://dx.doi.org/10.1016/j.toxlet.2007.01.008>
- 41 [Leavens, T; Borghoff, S](#). (2009). Physiologically based pharmacokinetic model of methyl tertiary
- 42 butyl ether and tertiary butyl alcohol dosimetry in male rats based on binding to
- 43 alpha2u-globulin. Toxicol Sci 109: 321-335. <http://dx.doi.org/10.1093/toxsci/kfp049>

- 1 [Licata, AC; Dekant, W; Smith, CE; Borghoff, SJ.](#) (2001). A physiologically based pharmacokinetic
2 model for methyl tert-butyl ether in humans: Implementing sensitivity and variability
3 analyses. *Toxicol Sci* 62: 191-204. <http://dx.doi.org/10.1093/toxsci/62.2.191>
- 4 [Mcgregor, D; Cruzan, G; Callander, R; May, K; Banton, M.](#) (2005). The mutagenicity testing of
5 tertiary-butyl alcohol, tertiary-butyl acetate and methyl tertiary-butyl ether in
6 *Salmonella typhimurium*. *Mutat Res* 565: 181-189.
7 <http://dx.doi.org/10.1016/j.mrgentox.2004.10.002>
- 8 [McGregor, DB; Brown, A; Cattanaach, P; Edwards, I; McBride, D; Caspary, WJ.](#) (1988). Responses
9 of the L5178Y tk+/tk- mouse lymphoma cell forward mutation assay II: 18 coded
10 chemicals. *Environ Mol Mutagen* 11: 91-118.
- 11 [Nihlén, A; Johanson, G.](#) (1999). Physiologically based toxicokinetic modeling of inhaled ethyl
12 tertiary-butyl ether in humans. *Toxicol Sci* 51: 184-194.
13 <http://dx.doi.org/10.1093/toxsci/51.2.184>
- 14 [Nihlén, A; Lof, A; Johanson, G.](#) (1995). Liquid/air partition coefficients of methyl and ethyl t-
15 butyl ethers, t-amyl methyl ether, and t-butyl alcohol. *J Expo Anal Environ Epidemiol* 5:
16 573-582.
- 17 [Nihlén, A; Lof, A; Johanson, G.](#) (1998a). Controlled ethyl tert-butyl ether (ETBE) exposure of
18 male volunteers: I Toxicokinetics. *Toxicol Sci* 46: 1-10.
19 <http://dx.doi.org/10.1006/toxs.1998.2516>
- 20 [Nihlén, A; Lof, A; Johanson, G.](#) (1998b). Experimental exposure to methyl tertiary-butyl ether: I
21 Toxicokinetics in humans. *Toxicol Appl Pharmacol* 148: 274-280.
- 22 [NIOSH](#) (National Institute for Occupational Safety and Health). (2007). NIOSH pocket guide to
23 chemical hazards. (2005-149). Cincinnati, OH. [http://www.cdc.gov/niosh/docs/2005-](http://www.cdc.gov/niosh/docs/2005-149/)
24 [149/](http://www.cdc.gov/niosh/docs/2005-149/)
- 25 [NSF International.](#) (2003). t-Butanol: Oral Risk Assessment Document (CAS 75-65-0). Ann Arbor,
26 MI.
- 27 [NTP](#) (National Toxicology Program). (1995). Toxicology and carcinogenesis studies of t-butyl
28 alcohol (CAS no 75-65-0) in F344/N rats and B6C3F1 mice (Drinking water studies) (pp.
29 1-305). (NTPTR436). Research Triangle Park, NC.
- 30 [NTP](#) (National Toxicology Program). (1997). NTP technical report on toxicity studies of t-butyl
31 alcohol (CAS no 75-65-0) administered by inhalation to F344/N rats and B6C3F1 mice
32 (pp. 1-56, A51-D59). Research Triangle Park, NC.
33 http://ntp.niehs.nih.gov/ntp/htdocs/ST_rpts/tox053.pdf
- 34 [OSHA](#) (Occupational Safety & Health Administration). (2006). Table Z-1 limits for air
35 contaminants. Occupational safety and health standards, subpart Z, toxic and hazardous
36 substances. (OSHA standard 1910.1000). Washington, DC: U.S. Department of Labor.
37 [http://www.osha.gov/pls/oshaweb/owadisp.show_document?p_table=STANDARDS&p](http://www.osha.gov/pls/oshaweb/owadisp.show_document?p_table=STANDARDS&p_id=9992)
38 [id=9992](http://www.osha.gov/pls/oshaweb/owadisp.show_document?p_table=STANDARDS&p_id=9992)
- 39 [Poet, TS; Valentine, JL; Borghoff, SJ.](#) (1997). Pharmacokinetics of tertiary butyl alcohol in male
40 and female Fischer 344 rats. *Toxicol Lett* 92: 179-186.
- 41 [Prah, J; Ashley, D; Blount, B; Case, M; Leavens, T; Pleil, J; Cardinali, F.](#) (2004). Dermal, oral, and
42 inhalation pharmacokinetics of methyl tertiary butyl ether (MTBE) in human volunteers.
43 *Toxicol Sci* 77: 195-205. <http://dx.doi.org/10.1093/toxsci/kfh009>

- 1 [Rao, HV; Ginsberg, GL.](#) (1997). A physiologically-based pharmacokinetic model assessment of
2 methyl t-butyl ether in groundwater for a bathing and showering determination. Risk
3 Anal 17: 583-598.
- 4 [Sgambato, A; Iavicoli, I; De Paola, B; Bianchino, G; Boninsegna, A; Bergamaschi, A; Pietroiusti, A;](#)
5 [Cittadini, A.](#) (2009). Differential toxic effects of methyl tertiary butyl ether and tert-
6 butanol on rat fibroblasts in vitro. Toxicol Ind Health 25: 141-151.
7 <http://dx.doi.org/10.1177/0748233709104867>
- 8 [Spiteri, NJ.](#) (1982). Circadian patterning of feeding, drinking and activity during diurnal food
9 access in rats. Physiol Behav 28: 139-147. [http://dx.doi.org/10.1016/0031-](http://dx.doi.org/10.1016/0031-9384(82)90115-9)
10 [9384\(82\)90115-9](http://dx.doi.org/10.1016/0031-9384(82)90115-9)
- 11 [Tang, G; Wang, J; Zhuang, Z.](#) (1997). [Cytotoxicity and genotoxicity of methyl tert-butyl ether
12 and its metabolite to human leukemia cells]. Zhonghua Yufang Yixue Zazhi 31: 334-337.
- 13 [U.S. EPA](#) (U.S. Environmental Protection Agency). (2000). Benchmark dose technical guidance
14 document [external review draft] [EPA Report]. (EPA/630/R-00/001). Washington, DC:
15 U.S. Environmental Protection Agency, Risk Assessment Forum.
16 <http://www.epa.gov/raf/publications/benchmark-dose-doc-draft.htm>
- 17 [Videla, LA; Fernández, V; de Marinis, A; Fernández, N; Valenzuela, A.](#) (1982). Liver
18 lipoperoxidative pressure and glutathione status following acetaldehyde and aliphatic
19 alcohols pretreatments in the rat. Biochem Biophys Res Commun 104: 965-970.
20 [http://dx.doi.org/10.1016/0006-291X\(82\)91343-2](http://dx.doi.org/10.1016/0006-291X(82)91343-2)
- 21 [Williams-Hill, D; Spears, CP; Prakash, S; Olah, GA; Shamma, T; Moin, T; Kim, LY; Hill, CK.](#) (1999).
22 Mutagenicity studies of methyl-tert-butylether using the Ames tester strain TA102.
23 Mutat Res 446: 15-21. [http://dx.doi.org/10.1016/s1383-5718\(99\)00137-0](http://dx.doi.org/10.1016/S1383-5718(99)00137-0)
- 24 [Williams, TM; Borghoff, SJ.](#) (2001). Characterization of tert-butyl alcohol binding to "alpha"2u-
25 globulin in F-344 rats. Toxicol Sci 62: 228-235.
- 26 [Yuan, Y; Wang, HF; Sun, HF; Du, HF; Xu, LH; Liu, YF; Ding, XF; Fu, DP; Liu, KX.](#) (2007). Adduction
27 of DNA with MTBE and TBA in mice studied by accelerator mass Spectrometry. Environ
28 Toxicol 22: 630-635. <http://dx.doi.org/10.1002/tox.20295>
- 29 [Zeiger, E; Anderson, B; Haworth, S; Lawlor, T; Mortelmans, K; Speck, W.](#) (1987). Salmonella
30 mutagenicity tests: III. Results from the testing of 255 chemicals. Environ Mutagen 9: 1-
31 60. <http://dx.doi.org/10.1002/em.2860090602>
32